Characterization of Micro Injection Molding Process for Milligram Polymer Micro Parts

N. Zhang & M.D. Gilchrist*

Mechanical & Materials Engineering, University College Dublin, Belfield, Dublin 4, Ireland

* Corresponding Author: michael.gilchrist@ucd.ie

Abstract

Injection molding small milligram components requires precise metering and high speed injection. Industrially, metering can be maintained either by using small injection screws (≤14mm in diameter) or plungers as small as 3mm diameter and/or by having very large sprues and runners. While large sprues and runners increase metering volume, they hide the effect of process parameters on micro components. Consequently, knowledge of conventional injection molding is not transferable to micro injection molding, making quality control and optimization difficult. We investigated the filling and post-filling behavior of 25mm^3 micro dumbbell specimens with 289 mm^3 sprue and runner by in-line process monitoring. Design of Experiments were carried out to characterize the effects of process parameters on cavity filling and post-filling behavior. Process characterization indicated that the machine transition from velocity control to pressure control (V-P transition) was around 10ms: this was comparable to cavity filling time and had a significant effect on cavity filling behavior. Traditional short shot trials cannot provide the correct shot size for small parts, but introduce the effect of holding pressure into cavity filling. Based on a shot size optimization method using only cavity pressure and screw velocity, we eliminated the effect of holding parameters on cavity filling.

1. Introduction

Micro injection molding is recognized as the most efficient production method to fabricate 3D polymer micro components weighing a few milligrams [1, 2] or parts having micro/nano scale features [3], such as micro gears [4] and microfluidic devices [5-8]. From a processing perspective, a decreasing cavity size poses challenges for filling the cavity, especially when its dimensions decrease to the micro/nano scale. Firstly, high speed injection and precise metering are essential for filling micro/nano cavities. Due to the high surface to volume ratio, micro parts and micro/nano scale features can solidify prematurely, causing problems of short shot. The molding process has to be finished as fast as possible. High speed injection can effectively reduce polymer melt viscosity by shear thinning and consequently decrease filling time significantly. Additionally, parts of only several cubic millimeters require precise metering of only a few milligrams of polymer. As a result, a micro injection molding machine must be equipped with a small diameter injection screw or plunger system in order to maintain the necessarily tiny metering volume. A high precision and fast response driven unit is also required to achieve high metering accuracy by precisely controlling the motion of the screw or plunger. Secondly, process consistency is of paramount importance for micro injection molding. Micro molded parts require extremely demanding tolerances, such as some optical components, up to ±3μm. A consistent process must ensure that all micro/nano features and tolerances are replicated properly and repeatedly. The larger metering tolerances of conventional injection molding (CIM) cause problems of consistency because of poor metering accuracy. Thirdly, extreme process conditions modify the microstructure and properties of polymers. Compared with conventional part, the surface to volume ratio of micro part and micro/nano scale features increases greatly, which means that surface physical phenomena are dominant. Filling of such small cavities needs high pressures and high temperatures in order to achieve fast injection. How this process influences the development of morphology is still not fully understood. Especially for replicating micro/nano surface features, the combination of all process parameters should ensure that the macro part has no defects such as short shot, thermal degradation or flash, and at the same time, ensure that the micro/ nano features are replicated with high quality and high consistency. How the best combination of process parameters can be obtained and assessed is still a problem that is faced by researchers and by industry.

Tremendous efforts have been made in the past 20 years and micro injection molding machines encompassing plunger, reciprocating-screw, and multi-stage styles, have been invented [1]. Because of the limitation of the size of polymer granules that are used in standard injection molding, the diameter of an injection screw cannot be smaller

than 14mm in diameter in order to maintain screw life and plastication efficiency [9]. Smaller injection screws struggles to maintain injection pressure and to feed polymer pellets. Typically, a Battenfeld Microsystem 50 has separate injection, metering and plasticizing units [10]. Its injection plunger diameter is 5mm and this means it can meter very small amounts of polymer melt, ~19.6 mm^3, when the plunger moves forward 1mm, equaling some 23mg of PMMA, which is even smaller than a standard PMMA pellet ~28mg. A conventional scale-down reciprocating injection molding machine equipped with a 14mm diameter injection screw can only meter as small as 153.9mm^3 for 1mm screw movement, i.e. around 183mg PMMA, which corresponds to ~6 standard polymer pellets. As a result, for such a tiny part, a molding machine with a large injection screw has no chance to inject material and switch over to the holding stage. Mold manufacturers usually design the sprue and runner system to be 100 times larger than the micro parts so that conventional industrial machines can control the metering volume. Although this can work, it is far from ideal because of problems of material waste, extended cycle time, possible degradation and process variation. Furthermore, it means that process parameters do not provide as much direct control or optimization of the required product properties as they would when regulating a large component. For example, tuning the process to adjust micro part morphology and to enhance the filling of micro/nano features is difficult, since the relatively large sprue and runner hide the effects of machine parameters on the micro part. In contrast to CIM, the morphology of micro injection molded parts has some unique features: a proportionally larger surface layer, a core with smaller diameter spherulites and even a spherulite-free core [11, 12]. These features result from high shear rates and high thermal gradients. Effectively, control and optimization are based on process characterization and this is key to controlling a product's final properties. Although this has been recognized, relatively little effort has been made to create process-specific and material-specific knowledge.

Several researchers have sought to monitor and characterise the micro injection molding process. Whiteside et al., [13, 14] monitored the injection pressure and cavity pressure using a Battenfeld Microsystem 50. The melt flow visualization, morphology, and mechanical properties were also analyzed at different process conditions. However, the cavity filling behavior and the relationship between process condition, cavity filling and microstructure have not been investigated. Chu et al., [10] also used a Battenfeld Microsystem 50 to systematically and quantitatively investigate the relationship between process conditions and cavity filling and packing behavior. However, due to space limitation in their mold cavity, cavity pressure sensors were not installed. They also did not investigate

machine dynamics. Griffith et al.[15] monitored cavity air flow behavior and provided empirical evidence on the effects of process parameters on cavity air evacuation, and the influence of air evacuation on the part flow length.

In our previous work, we characterized the thermo-rheological behavior of polymer under real micro injection molding process conditions [16]. The present paper will focus on process characterization of a reciprocating micro injection molding system with a 14mm diameter injection screw for typical micro component that has a larger sprue and runner. Process conditions that the materials experience will be monitored by an in-line pressure and temperature measurement system. Firstly, conventional short shot trials will be used to optimize the shot size for each process condition; gate solidification time will be estimated using cavity pressure curves; the effect of machine process parameters on the filling, packing and cooling stages will be analyzed statistically using process characteristic values (PCVs). The dynamic response of the machine and its resulting effects on cavity filling will also be characterized. As a result of this analysis, we propose a new method for shot size optimization based on the in-line monitored cavity pressure and screw position. The effect of machine process parameters on PCVs will be analyzed to validate that the process is under control and can be optimized.

2. Experimental methods

2.1 Machine, mold and material

All the experiments were implemented using a Fanuc Roboshot S-2000i 15B reciprocating micro injection molding machine, which was equipped with a 14mm diameter injection screw. Two dumbbell mold inserts were designed to form cavities with depths of 500 and 400 μm, both having micro/nano scale features. The total volume of sprue, runner, and gate was 289 mm^3, which was ~11.5 times larger than the 500μm thick dumbbell part (25mm^3). The molded part and its detailed dimensions are displayed in Fig. 1. High density polyethylene (HDPE HMA016 grade, ExxonMobil, MFI 20g/10min, ASTM D1238) and Cyclic Olefin Copolymer (COC 5013L10, Topas, MVR 48cm^3/10min, ISO1133) were used as molding materials.

2.2 Process monitoring system

Two Kistler 6189A combined pressure and temperature sensors (PT sensors) were fitted into the waisted regions of the dumbbell mold cavity so as to directly detect the melt temperature and cavity pressure at the same position, as

shown in Fig. 1(d) and Fig. 2 (a). A Kistler COMO injection process monitoring system (2869B) was used for data acquisition (Fig. 2 (b)). Cavity pressure and material contact temperature were firstly collected by COMO and then were outputted into a computer by Ethernet. Additionally, injection velocity, injection pressure and screw position during the injection molding process were also outputted into the COMO system. Injection signals from the molding machine triggered COMO to ensure that all the signals were received simultaneously.

2.3 Experimental design

Design of Experiment (DOE) was used to analyze the effects of machine parameters on process conditions. The following machine parameters were selected: injection velocity (V_i), holding pressure (P_h), holding time (t_h), barrel temperature (T_b) and mold temperature (T_m). Two level half factorial designs (2^{5-1} and 2^{4-1}) were conducted for both HDPE and COC, as shown in Table 1. All process conditions were randomly repeated 3 times for HDPE and 2 times for COC according to the internal random function of the Minitab software. The velocity pressure switchover position of the machine was set at 5mm for all process conditions. A traditional short shot method was used to optimize shot size for HDPE. The displacement increment was set as 0.02mm and the corresponding volumetric increment was 3.077mm^3. Shot size for COC was optimized based on screw velocity and cavity pressure, which is discussed in detail in Section 3.3.2.

3. Results and discussion

3.1 Cavity filling behavior

The filling stage is of great importance in the micro injection molding process, in which polymer melt is injected into a mold cavity to fill the mold cavity and surface micro/nano features. A fast solidification layer forms immediately when hot melt contacts a relatively cold cavity wall. Micro/nano features, particular those that have similar dimensions to the skin layer, are formed mainly in this stage. In addition, high shear rates during filling have a significant effect on the molecular orientation and this will ultimately influence anisotropy and mechanical properties of micro parts [17].

3.1.1 Cavity filling

As shown in Fig. 3, screw position, injection pressure, cavity pressure and material contact temperature of the mold-polymer interface under process condition 10 were monitored for 5s after injection. The trace curves of the first 0.1s were enlarged to make the filling stage more clearly visible, as shown in Fig. 4. At the beginning, the injection screw moves forward with no significant pressure rise during the first 5ms. This is probably due to a small flow resistance after decompression in the plastication stage. The small rise of injection pressure and screw position, at 0.017s, indicates that the melt front starts to fill the runner. The volume filling the sprue is around 190mm^3, which corresponds to 1.47mm of screw forward displacement. The corresponding metering volume is 226mm^3, which is almost 19% higher than the volume of the sprue, as calculated from the 3D geometric model. This larger difference is because of the P-v-T behavior of the polymer melt and also because of material being lost due to leakage from backflow from the injection nozzle. A similar phenomenon is seen when filling the runner, gate and cavity. The screw, runner and part of the cavity are filled before sensor 1 registers any signals. The material contact temperature of sensor 1 is higher than that of sensor 2. This is probably due to heat loss at the melt front when melt travels from sensor 1 to sensor 2. Sensor 1 registers pressure and temperature at the same time, around 34ms after injection, as shown in Fig. 4. The material contact temperature at the position of sensor 1 is significantly lower than would be expected, partly because the thermocouple needs time to track the real temperature. Possible jetting problems reported for HDPE [11] could also partly explain this temperature. The temperature at sensor 1 is the material temperature at the skin layer of a jetting flow and this increases with time while heat transfers from the core region to the mold wall. Around 8ms later, sensor 2 registers pressure and temperature signals. Both the jump of cavity pressure sensed by sensors 1 and 2 and injection pressure at 0.056s indicate that the cavity is almost fully filled, at which stage the screw position is 3.21mm. The entire corresponding displacement of the screw during the filling stage is approximately 6.29mm and the corresponding volume is 969mm^3, which is 32% larger than the entire volume of the whole molded part. This difference could be due to the P-v-T behavior of the material.

Because the dumbbell sample is symmetric about its middle axis, the volume of material between the gate and sensor 1 is equal to that between sensor 2 and the end of the sample. As a result, the screw displacement to fill the volume from sensor 2 to the sample end is about 0.75mm, which is approximately equal to the corresponding screw displacement (Δd) to fill the volume from the gate to sensor 1. Thus, the corresponding time at which the cavity starts filling is determined as ~0.029s. Based on the P-v-T data [18] and considering the influence of pressure inside the cavity during cavity filling, the error in this estimated screw position is around 4%. In summary, mold filling is

triggered by the injection signal. The sprue is filled after around 0.017s. After that, the melt keeps moving forward to fill the runner and gate. The estimated time at which cavity filling starts is 0.029s. The cavity filling takes around 0.027s.

3.1.2 V-P switchover

In conventional injection molding, the cavity volume is large enough that any effects of switchover from velocity control to pressure control (V-P switchover) on the cavity filling behavior are negligible. However, as discussed in Section 3.1.1, the cavity filling time is only 0.027s and the V-P switchover could influence cavity filling. In the present study, metering size was considered as a variable and was optimized by short shot trials for each process condition in order to obtain a uniform switchover position. The typical position switchover method was adopted, with the set mechanical switchover position being 5mm in all the experiments. The actual switchover positions of 100 cycles for the same process conditions were output from the machine database, as shown in Fig. 5. The average switchover position was 4.97mm with a standard deviation of 0.063, which corresponded to the switchover time of 33ms after injection. The coefficient of variation is 1.26%, which proves that the machine is under control. Fluctuations of the V-P position might be caused by factors such as non-homogenous material properties and machine control mechanism, metering size and back flow. In fact, the set injection velocity was not actually reached within around 33ms after start of injection to the switchover position. The actual peak injection speed was around 220mm/s under process condition 10. The velocity build up depends on the dynamics of driven motors and the selected dynamic response style, control unit etc.

The experiments of process condition 10, with and without packing pressure, were implemented to investigate the transition from velocity control to pressure control. Figure 6 displays the profiles of cavity pressure, injection pressure, screw position and screw injection velocity for process condition 10, i.e., with and without packing pressure. The set switchover position was 5mm, as shown by the dash dotted line at position B. The corresponding injection pressure was around 43MPa, while the corresponding injection velocity reached its maximum and decreased quickly after this point. This indicates that the machine started the V-P transition from its switchover position. When the screw reached position D, i.e., at 3.5mm, the response of both the injection pressure, screw position and screw velocity diverged from each other: this indicates that the transition from velocity control to pressure control was completed and the pressure control started taking effect. The period of time during which the screw travelled from position B to position D was defined as the V-P transition time and it was ~10ms. The

corresponding screw displacement was around ~1.5mm, which is the so-called deceleration stroke. The corresponding deceleration volume was ~231mm^3. The V-P transition is an inherent characteristic of an injection molding machine. The transition time was assumed to be constant for all process conditions in the present study. It is worth noting that the cavity was not fully filled before the V-P transition when the screw was held at position B. The corresponding cavity pressure was around 12 MPa, as shown at point C. The actual cavity filling continued with the transition from velocity control to pressure control.

3.1.3 Process characteristic values (PCVs) in filling stage

The filling stage was characterized by selected PCVs. Average screw velocity and average injection pressure during the cavity filling stage were used as PCVs to describe dynamic machine responses during the cavity filling process. As cavity pressure is sensitive to changes in injection pressure, injection rate, screw speed, back pressure and cushion [19], the average cavity pressure was adopted as a process characteristic value. By using the method that was adopted to estimate the corresponding screw position at the beginning of cavity filling, the start time for cavity filling could be determined. Based on the length of the tensile sample, the average filling velocity was calculated as another process characteristic value. The average cavity pressure and filling velocity provide the insight into the actual cavity filling process. This work also used the predetermined metering size as a process characteristic value, which determined the amount of material that was injected into the mold.

3.2 Post filling behavior

Post filling commences as soon as the cavity is completely filled. It is controlled by heat transfer in the mold cavity and by compressibility of the solidifying melt. During holding, the injection pressure changes rapidly to the set holding pressure and is held for a short interval. After gate solidification, material is locked inside the cavity and remains physically isolated from the injection molding machine. Pressure and temperature follow a monotonic decay until the end of the cycle, after which the polymer has solidified and is ejected out of the mold. The final properties of injection molded parts, such as the microstructure, birefringence, the presence of residual stresses, density fluctuations, any shrinkage or warpage of the parts, are closely related to the holding and cooling conditions [20].

3.2.1 Gate solidification time

Estimating the actual gate solidification time is important so as to distinguish between holding and cooling. Krug et al. [21] and Pantani et al. [22] estimated the gate solidification time based on an inflection point in the cavity

pressure curves. As shown in Fig. 7, dp/dt is a monotonically decreasing function up to ~0.3s and a monotonically increasing function after ~0.3s. This indicates that the inflection happened at ~0.3s. The corresponding weight of parts is also essentially stable when the holding time exceeds ~0.3s, as indicated in Fig. 7 (b), which suggests that the gate has solidified and no further polymer can be packed into the cavity. The inflection of the cavity pressure verse time curve will be used as a sign of gate solidification to identify holding and cooling stages. In addition, when the holding time is shorter than the gate solidification time of ~0.3s, the cavity pressure decays very quickly at a holding time of 0.2s, as shown in Fig. 7 (a) for the case with a holding time of 0.2s. On the other hand, when the holding time exceeds ~0.3s, cavity pressure remains very consistent.

3.2.2 Holding and cooling behavior

Figure 8 shows trace curves of injection pressure, screw position, cavity pressure, and material contact temperature. After 0.056s from the beginning of injection, the cavity is fully filled and injection and cavity pressure significantly increase to the set holding pressure of 70MPa after 0.1s. The injection pressure and cavity pressure maintain a constant value for 0.15s and then decay gradually. In this process, some extra material is forced into the mold to compensate for shrinkage from the solidification process. However, displacement of the screw position, which controls the amount of material packed into the cavity, is not so significant, due to a small cavity and large injection screw. Normally, holding pressure is maintained until the gate solidifies and no more material is allowed to enter or exit the mold cavity. However, under process condition 10, the holding time (~0.2s) is shorter than the estimated gate solidification time (~0.3s). The cavity pressure measured at sensor 2 near the part end exceeds that of sensor 1 near the gate. This pressure difference leads to back flow inside the cavity and some material could even exit the cavity. This would give rise to an object that is lighter and smaller and has a different morphological distribution.

The contact temperature distributions of sensor 1 and sensor 2 recorded over 5s following injection, are shown in Fig. 3. The recorded temperatures quickly reach the maximum values at 0.27s, which corresponds to the time that the sensor starts to track the temperature. This coincides with the response time of the sensors. Due to fast filling and the relatively slow response time of the temperature sensors, it is impossible to monitor temperature distribution in the filling stage. The cooling stage occurred after gate sealing; the cavity pressure then decays gradually and it is the P-v-T behavior of the material that determined the cavity pressure and final dimensional accuracy. Cavity pressure finally decays to 0MPa at ~0.6s, which indicated that the polymer detached from the mold surface. Because the

cooling rate of the part varies from the core to the skin, the nominal cooling conditions could be only evaluated by the degree of supercooling [23], which depends on mold-polymer interface temperature and melt temperature. As a result, peak injection pressure, peak cavity pressure, peak material contact temperature, gate solidification time and screw displacement were selected as PCVs of the post-filling stage. Five consecutive cycles of each process condition were selected to obtain the process characteristic values.

3.3 Process characterization

3.3.1 HDPE

3.3.1.1 Filling

Figures 9 (a) and (b) display the mean and standard deviation of the defined process characteristic values during the cavity filling process under different process conditions. The average injection velocity ranges from its lowest value of ~70mm/s at process conditions 1, 5, 9 and 13 to its highest value of ~205 mm/s at process conditions 4, 8, 12, and 16, as shown in Fig. 9 (a). Compared to cases of lower injection velocity settings (100mm/s), the average injection velocity of the cases with high injection velocity setting (450mm/s) are far lower than the set injection velocity. This indicates that the screw velocity does not fully build up at the high injection velocity settings: this is because of the slow dynamic response of the injection server motor [24]. The metering size displays the exact opposite trend i.e., the metering size increases with lower injection velocity. Meanwhile, for the same setting of injection velocity, the metering sizes are higher for cases with lower mold and melt temperatures. The variations of metering size indicate that the metering size is primarily dominated by injection velocity and by mold and melt temperature. This is explained by viscous dissipation caused by high shear rates, and the P-v-T behavior of the material. As shown in Fig. 9 (b), the average filling velocity and average cavity pressure display a similar pattern. The actual average cavity pressure ranges from 20.8MPa to 24.8MPa. The maximum and minimum average cavity filling velocities are ~1200mm/s and ~500mm/s, respectively. Based on Newtonian flow, the corresponding shear rates range from $2500s^{-1}$ to $6000s^{-1}$. This is directly associated with shear induced crystallization. Compared to PCVs for machine response and for cavity filling from both Fig. 9 (a) and (b), it can be seen that the average filling velocity has a similar distribution to that of the average screw velocity. Average filling velocity also presents a similar pattern with average cavity pressure, which indicates that an increasing screw velocity can lead to a rise of cavity pressure.

Figure 10 shows the standardized effects of the machine parameters and their interactions on process characteristic values. Injection velocity is the main positive factor to influence average cavity pressure. Melt temperature and mold temperature both have a negative effect on the average cavity pressure, which is closely associated with the shear thinning behavior of HDPE and flow resistance of the cavity. Both the injection velocity, melt temperature and mold temperature have a negative effect on the metering size. The holding pressure, melt temperature and mold temperature exert a negative effect on the average injection pressure. It is for this reason that the average injection pressure presents a complex pattern in Fig. 9 (a). As shown in Fig 10, injection velocity, holding pressure, melt temperature and mold temperature all show positive effects on the average filling velocity. Similarly, both the injection velocity and holding pressure have positive effects on the average screw velocity.

It needs to be emphasized that the filling stage is also affected by holding pressure, based on statistical analysis. In order to analyze the effect of holding pressure on filling behavior, two process conditions, cases 10 and 16 with 70MPa and 120MPa holding pressures respectively, are compared, as shown in Fig. 11. These two conditions have the same machine parameters except for holding pressure and holding time. The holding time is not considered due to its small effect on the filling stage.

Here we divide the cavity filling stage into two sub-stages: cavity filling before and after the V-P transition is complete. The estimated time at which the filling starts is around 0.032s for process condition 10, as shown in Fig. 11(a). The corresponding screw position is around 5.7mm. The switchover position is around 5mm, as indicated in Section 3.1.2. Assuming the V-P transition time is consistently 10ms, the estimated V-P transition starts at 0.034s and finishes at 0.044s for case 10. However, the cavity is not fully filled at 0.044s and the injection screw is still moving forward to fill the rest of cavity until 0.053s, at which time the cavity is fully filled with a significant increase of cavity pressure, as shown in Fig. 11 (a). Consequently, the filling behavior is actually controlled by the holding pressure after the V-P transition. Similarly, the estimated V-P transition finishes at 0.043s for case 16, as shown in Fig. 11 (b). The cavity is fully filled after 0.045s. As a result, cavity filling of process condition 16 is also affected by the holding pressure. However, the time to fill the cavity under holding pressure control lasts for only 3ms for process condition 16, and for around 11ms for case 10. This is because the set holding pressure for case 16 is higher than that for case 10. The higher holding pressure requires that the injection screw moves faster to achieve its set value. The corresponding average screw velocity is 350mm/s for case 16, which is faster than the 49mm/s for case 10 after the V-P transition. The corresponding screw displacement is 0.7mm (for a volume of 108mm^3) and

0.5mm (for a volume of 78mm^3) for cases 16 and 10, respectively. Obviously, the average screw velocity and filled volume of case 16 after the V-P transition and before full filling is significantly higher than that associated with lower holding pressure for case 10, due to high inertia from the high velocity. The corresponding filling time of case 16 is significantly shorter than that of case 10. In all, the V-P transition in the micro injection molding process is ~10ms, which is comparable to the cavity filling time (16~22ms) and this transition means that holding pressure significantly affects the cavity filling behavior.

3.3.1.2 Post filling

As shown in Fig. 12, peak cavity pressure and peak injection pressure have a similar pattern and do not change with the polymer mold interface temperature, which follows the variation of holding pressure. But both the barrel and mold temperature have a significant effect on cavity pressure. This is because the cavity is so small and variations induced by temperature would lead to significant changes, but it is not large enough to change the injection pressure. The screw displacement in Fig. 12 (b) follows a similar pattern to peak cavity pressure, although the material temperature changes significantly at different process conditions. This indicates that screw displacement during the holding stage depends mostly on pressure, in contrast to temperature. This is consistent with the statistical analysis shown in Fig. 13, which indicates that holding pressure almost dominates screw displacement, although barrel temperature and molding temperature are also significant factors that influence screw displacement. Gate sealing time varies significantly with process conditions, but has no dependence on cavity pressure and temperature. It has been reported that gate thickness and cavity geometry are the most important factors in determining gate sealing time [25]. The present statistical analysis implies that all process parameters have a significant effect on gate sealing, as shown in Fig. 13 (b). Holding pressure has the most negative effect and mold temperature and holding time have the most positive effect. The effect of holding pressure and holding time can be explained by the variation in the heat transfer coefficient with pressure and time [20].

3.3.2 COC

3.3.2.1 Shot size optimization based on screw velocity

Proper determination of switchover from velocity control in the filling stage to pressure control in the holding stage can reduce defects from over-packing and under-packing, such as flash, sticking to mold, breakage due to higher residual stress, sink marks and underweight [26]. Switchover time, ~10ms, is much shorter than the filling time for

conventional injection molding and is usually ignored. However, for micro injection molding, such small part volumes make the filling time comparable to the machine switchover time. The switchover time would consequently have a significant influence on the filling or packing process, as observed during the HDPE filling process described in Section 3.3.1.

The ideal switchover position ought to be indicated by a significant increase of cavity pressure when the polymer melt reaches the end of the cavity. Based on observations of cavity pressure with the current process monitoring system, we developed a shot size optimization method to ensure the correct switchover. The switchover position was set as 5mm. It is known that once the machine switches from filling to packing, screw velocity drops rapidly until the screw pressure reaches the set holding pressure. Therefore, screw velocity was used as an indicator for the switchover transition. The shot size is gradually increased until screw velocity falls down at the same time that cavity pressure significantly increases. COC was used as an example to optimize the shot size based on cavity pressure and screw velocity. Figure 14 shows cavity pressure, injection velocity, and screw position after shot size optimization with and without holding stage using this method. It can be seen in the full shot without holding stage, that the machine switches over at 0.075s with the switchover position ~3.6mm, at which time cavity pressure increases significantly. When a holding stage was included into the process under the same condition, the machine switches over at 0.065s, with the corresponding switchover position of 4.82mm. Assuming the V-P transition is ~10ms, it is seen that the machine switchover happens between 0.065s and 0.075s, which ideally diminishes the effect of holding pressure on the filling process. This method was used to optimize shot size for all process conditions for COC.

3.3.2.2 Filling

The variation of PCVs with different process conditions for COC is shown in Fig. 15. In contrast to HDPE, the variation of metering size is not significant. From the statistical analysis of Fig. 16, mold temperature is the most significant factor and this has a negative influence on shot size, although injection velocity also has a significant effect. This diverges with HDPE, which depends on material P-v-T property. As shown in Fig. 15, the average screw velocity reaches almost the maximum level at process conditions 2, 4, 6 and 8, i.e., a high injection velocity ~200mm/s, and reaches the minimum level for process conditions 1, 3, 5 and 7, i.e., a low injection velocity ~100mm/s. Obviously, the set maximum velocity of 250mm/s (high level) is not achieved because of the short filling time, which is similar to HDPE. However, for the 100mm/s low velocity setting, it is fully achieved.

Statistical analysis in Fig.16 indicates that screw velocity is fully determined by the injection velocity setting. This indicates that the process is under control and low injection velocity settings can be achieved very well for micro injection molding. The average injection pressure does not change much under the selected process conditions. It is found that mold temperature is the most significant negative factor influencing injection pressure and the interaction of injection velocity and holding pressure is the most significant positive factor.

With respect to filling conditions in the micro cavity, cavity pressure did not change very much with the maximum pressure being ~10MPa, which was much lower than the maximum injection pressure ~50MPa. This indicates that the pressure drop is quite significant during the cavity filling process. This could be addressed to obtain a high cavity pressure for filling micro/nano features either by reducing the flow length of the sprue and runner or by increasing the gate size. From a processing perspective, statistical analysis indicates that the interaction of injection velocity and mold temperature determines the cavity pressure. A high mold temperature would prevent the polymer from premature solidification, which is identified as the most significant factor to affect micro/nano surface feature replication [27]. An increase of cavity pressure can also force more polymer into a micro/nano cavity by either viscous flow or short term creep [28].

The average cavity filling velocity has a similar pattern to the average screw velocity and has the maximum velocity of ~900mm/s (corresponding to shear rate is ~4500s^{-1}) and the minimum velocity of ~400mm/s (shear rate is ~2000s^{-1}); this is much higher than the actual screw velocity, because the reduced cavity volume induces an increase in volume flow rate. Statistical analysis also indicated that cavity filling velocity is determined by the set injection velocity.

3.3.2.3 Post-filling

As shown in Fig. 17, peak injection pressure and peak cavity pressure present similar patterns of variation to that of the average screw velocity shown in Fig. 15. This indicates that peak injection pressure and cavity pressure both influence injection velocity. Statistical analysis indicates that injection velocity is the most significant positive factor on peak cavity pressure, and mold temperature is the most significant negative factor. As shown in Fig. 14, after the V-P transition, screw velocity does not reduce to zero immediately. It continues moving forward under inertia and pushes more material into the cavity, leading to a significant increase of cavity pressure and injection pressure. This process was influenced by the set injection velocity, temperature and machine dynamic response.

For polymer-mold contact temperature, process conditions 1, 2, 5 and 6 have the minimum value of ~120^{o}C at the lowest mold temperature setting and 3, 4, 7 and 8 have the maximum temperature of ~140^{o}C at the highest temperature settings. Mold temperature dominates the interface temperature, indicated by statistical analysis, shown in Fig. 18 (a). Gate sealing time depends on the thermo-mechanical history of material during the entire process. Statistical analysis indicates that all selected parameters have a significant effect on gate sealing, as shown in Fig. 18 (b), which is similar to HDPE. Screw displacement in the holding stage is determined by holding pressure and mold temperature, which is as it should be and confirms that the holding phase is totally controlled by holding pressure. The holding time has no significant effect on screw displacement. This is because the maximum gate sealing time is ~0.3s, which is well below the set holding times of 0.5s and 1s. In summary, the post-filling stage is well controlled by both holding pressure and mold temperature.

4. Conclusions

Polymer micro components weighing up to a few milligrams are particular challenging for precise metering and injection, mold fabrication, process control and optimization, quality inspection and numerical simulation. Usually, during industrial production, a small injection screw or plunger is used to meter and inject a precise amount of polymer into the mold. Additionally, a larger sprue and runner are also designed to increase shot volumes so as to preserve metering precision. The small volumes of the micro parts also makes cavity filling and cooling very fast. This requires injection molding machinery to have a very fast injection velocity and consequently this means that material experiences very high shear rates. The corresponding process-specific knowledge required for such components is rare and makes process based quality control and optimization quite difficult.

In the present work, we used a reciprocating micro injection molding machine with a 14mm diameter injection screw to mold 25mm^3 dumbbell specimens. Cavity filling and post-filling behavior were analyzed based recorded cavity pressure and mold polymer interface temperature, injection pressure, screw position and screw velocity. Some unique features have been found for this micro injection molding process. Firstly, the cavity filling time was around 16~24ms, which was similar to the machine V-P transition time of ~10ms. It was found that the V-P transition had a significant effect on cavity filling behavior. Traditional short shot trials cannot provide the correct shot size for small parts, but introduce the effect of holding pressure into cavity filling. Secondly, although the machine was under

control, the injection velocity, set at high level, could not be achieved, because of the short filling time and slow machine dynamic response.

Process characteristic values were selected to characterize the filling and post-filling stages. For HDPE, traditional short shot trials was used to optimize shot size and statistical analysis indicated that metering size was determined by injection velocity, mold temperature and melt temperature, depending on the P-v-T behavior of materials. Cavity filling behavior was determined by injection velocity and holding pressure. Machine response at the filling stage was both controlled by injection velocity and holding pressure. Screw displacement was determined by holding pressure, and by mold and melt temperature at post-filling stage. All process parameters have an effect on the gate sealing time for HDPE and COC, because of the materials' thermo-mechanical histories during the molding process. The polymer-mold interface temperature is fully governed by mold temperature. Based on monitored cavity pressure and screw velocity, we optimized shot sizes for COC to ensure that the V-P transition occurred immediately before the holding stage so as to eliminate any effects of the holding stage on the cavity filling behavior. Statistical analysis indicated that the effect of holding pressure on filling was eliminated after the shot size was optimized with the proposed method. This provides a basis for process control and optimization for such small milligram parts.

Acknowledgement

The authors gratefully acknowledge financial support from Enterprise Ireland (Grant Nos. CFTD/07/314 and CF/2012/2022), the Chinese Scholarship Council, and University College Dublin. We also acknowledge Dr. Jingsong Chu (now President of Micromoulding Solutions Inc., Canada) for designing the mold and the inserts and also discussions regarding process characterization of HDPE.

References

1.G. Julien, C. Thierry, M. Patrice, *J. Micromech. Microeng.*, **17** , 96 (2007).

2. U. Attia, S. Marson, J. Alcock, *Microfluid. Nanofluid.*, **7** , 1 (2009).

3. N. Zhang, C.J. Byrne, D.J. Browne, M.D. Gilchrist, *Mater. Today*, **15**, 216 (2012).

4. S. Yuan, N.P. Hung, B.K.A. Ngoi, M.Y. Ali, *Mater. Manuf. Process.*, **18** , 731 (2003).

5. S. Haeberle, R. Zengerle, *Lab. Chip.*, **7** 1094 (2007).

6. S. Choi, D. Kim, T. Kwon, *Microsyst.Technol.*, 15, 309 (2009).

7. D.A. Mair, E. Geiger, A.P. Pisano, J.M.J. Frechet, F. Svec, *Lab. Chip.*, **6** ,1346 (2006).

8. U. Attia, J. Alcock, *Int. J. Adv. Manuf. Technol.*, **48** , 973 (2010).

9. W. Michaeli, A. Spennemann, R. Gärtner, *Microsyst. Technol.*, **8** , 55 (2002).

10. J. Chu, M.R. Kamal, S. Derdouri, A. Hrymak, *Polym. Eng. Sci.*, **50** , 1214 (2010).

11. M. R. Kamal, J. Chu, S. Derdouri, A. Hrymak, *Plast. Rubber. Compos.,* **39**, 332, (2010).

12. J. Giboz, A. B. Spoelstra, G. Portale, T. Copponnex, H. E. H. Meijer, G. W. M. Peters, P. Mélé, *J. Polym. Sci. Pol. Phys.*, **49** 1470 (2011).

13.B.R. Whiteside, M.T. Martyn, P.D. Coates, G. Greenway, P. Allen, P. Hornsby, *Plast. Rubber. Compos.*, **33** , 11 (2004).

14.B.R. Whiteside, R. Spares, K. Howell, M.T. Martyn, P.D. Coates, *Plast. Rubber. Compos.*, **34** ,380 (2005).

15.C.A. Griffiths, S.S. Dimov, S. Scholz, G. Tosello, *J. Manuf. Sci. Eng.*, **133** ,011006 (2011).

16.N. Zhang, M.D. Gilchrist, *Polym. Test.*, **31**, 748 (2012).

17. H. Ben Daly, K. T. Nguyen, B.Sanschagrin, K.C.Cole, *J. Inject. Mold. Technol.*, **2** , 59 (1998).

18. S. Chakravorty, *Polym. Test.*, **21**, 313 (2002).

19. D.V.R. Dominick V. Rosato, Marlene G. Rosato, *Injection Molding Handbook*, 3 ed., Kluwer Academic Publishers, London (2000).

20. G.T. Roberto Pantani, *Modelling aspects of post-filling steps in injection molding,* M. R. Kamal, S. Liu (Ed.) *Injection molding: technology and fundamentals*, Hanser Publications, Munich (2009).

21. S. Krug, J.R.G. Evans, *Ceram. Int.*, **25** , 661,(1999).

22. R. Pantani, F. De Santis, V. Brucato, G. Titomanlio, *Polym. Eng. Sci.*, **44** ,1,(2004).

23. J.C. Viana, A.M. Cunha, N. Billon, *Polym.*, **43**, 4185, (2002).

24. Y.-B. Bang, S. Ito, *P. I. Mech. Eng. B.-J. Eng.*, **216,** 773,(2002).

25. R. Pantani, V. Speranza, G. Titomanlio, *Polym. Eng. Sci.,* **41** ,2022, (2001).

26. M.-S. Huang, *J. Mater. Process. Technol.*, **183** , 419, (2007).

27. N. Zhang, J.S. Chu, C.J. Byrne, D.J. Browne, M.D. Gilchrist, *J. Micromech. Microeng.*, **22** ,065019 (2012).

28. M. Yoshii, H. Kuramoto, K. Kato, *Polym. Eng. Sci.*, **34** ,1211,(1994).

Table 1. Experimental design matrix for HDPE and COC

Material	Process conditions	V_i(mm/s)	P_h(MPa)	t_h(s)	T_b(^{o}C)	T_m(^{o}C)
HDPE	1	100	70	0.2	150	70
	2	450	70	0.2	150	40
	3	100	120	0.2	150	40
	4	450	120	0.2	150	70
	5	100	70	0.6	150	40
	6	450	70	0.6	150	70
	7	100	120	0.6	150	70
	8	450	120	0.6	150	40
	9	100	70	0.2	160	40
	10	450	70	0.2	160	70
	11	100	120	0.2	160	70
	12	450	120	0.2	160	40
	13	100	70	0.6	160	70
	14	450	70	0.6	160	40
	15	100	120	0.6	160	40
	16	450	120	0.6	160	70
COC	1	100	70	0.5	N/A	95
	2	250	70	1.0	N/A	95
	3	100	70	1.0	N/A	115
	4	250	70	0.5	N/A	115
	5	100	90	1.0	N/A	95
	6	250	90	0.5	N/A	95
	7	100	90	0.5	N/A	115
	8	250	90	1.0	N/A	115

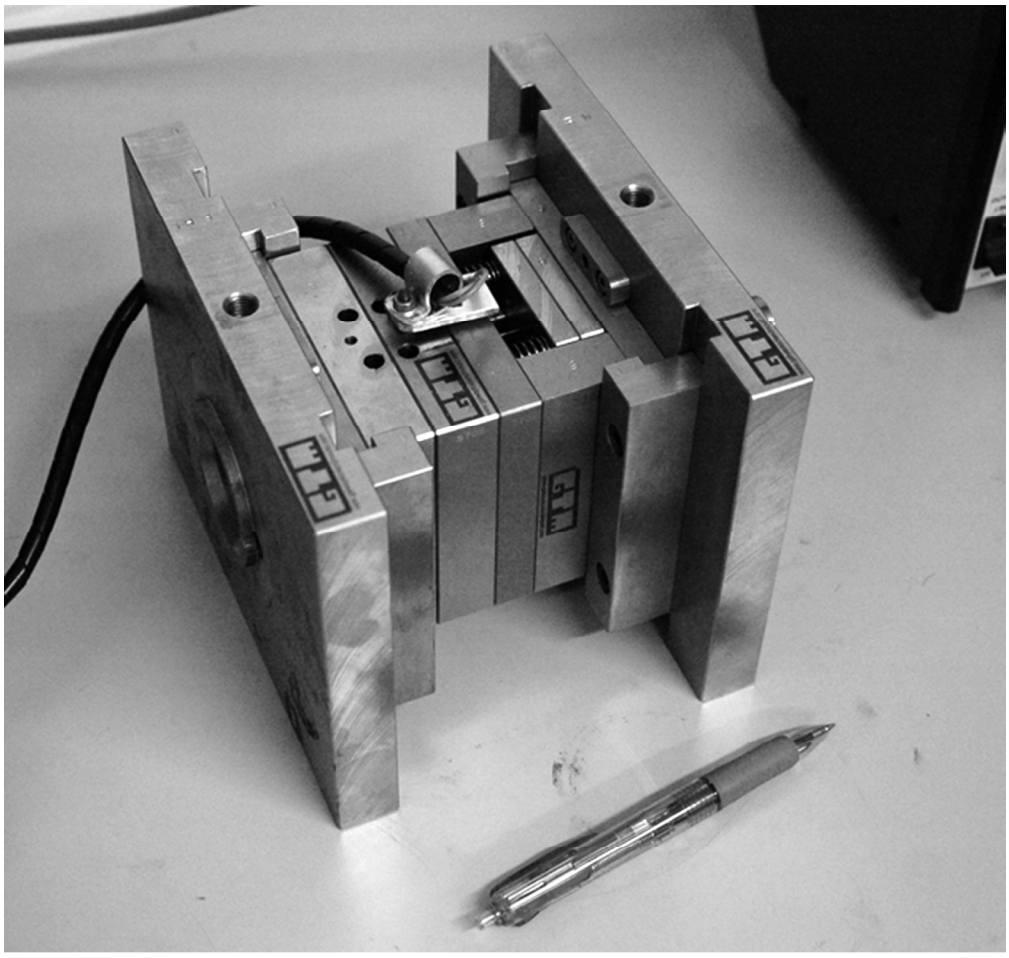

Figure 1: Mold and part: (a) mold
80x75mm (300 x 300 DPI)

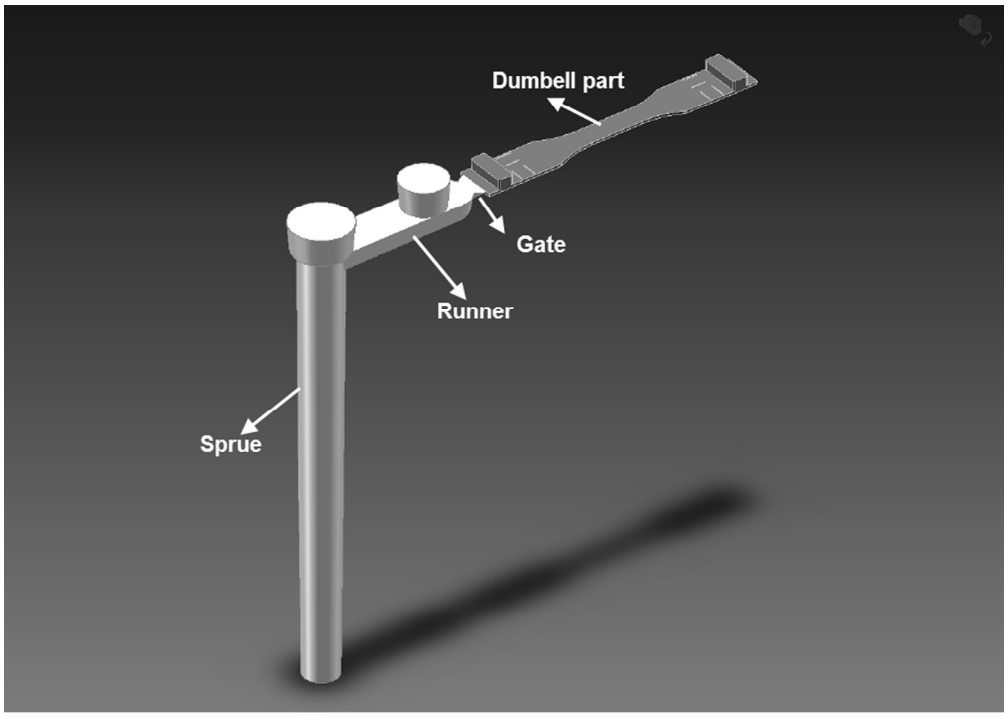

Figure 1: Mold and part: (b) geometrical model of dumbbell specimen with larger sprue, runner and gate
192x135mm (300 x 300 DPI)

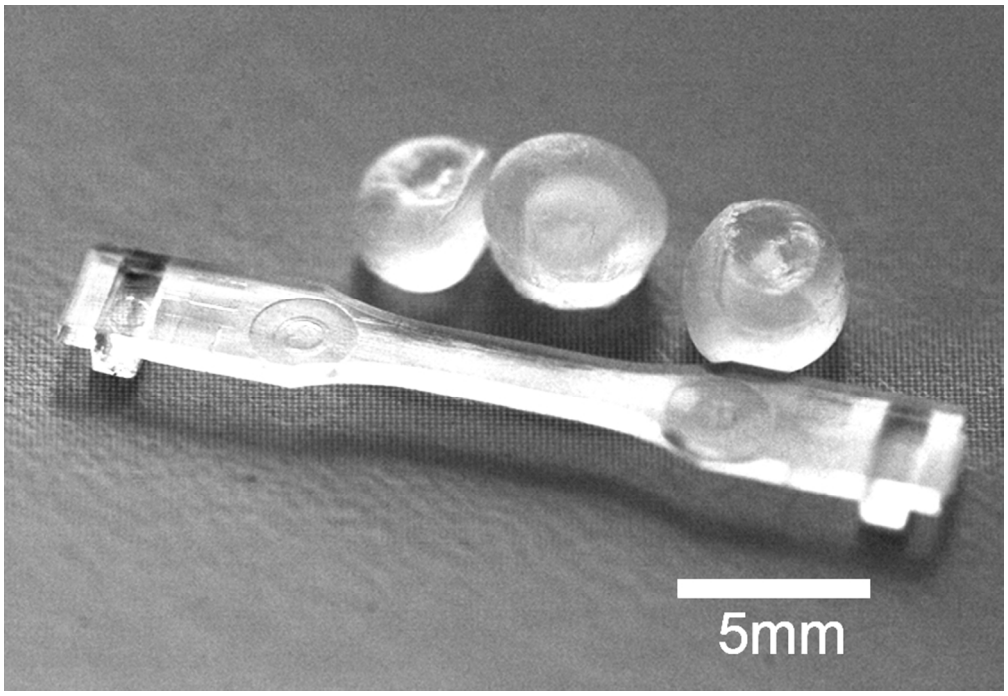

Figure 1: Mold and part: (c) molded micro component with standard polymer pellets
84x57mm (300 x 300 DPI)

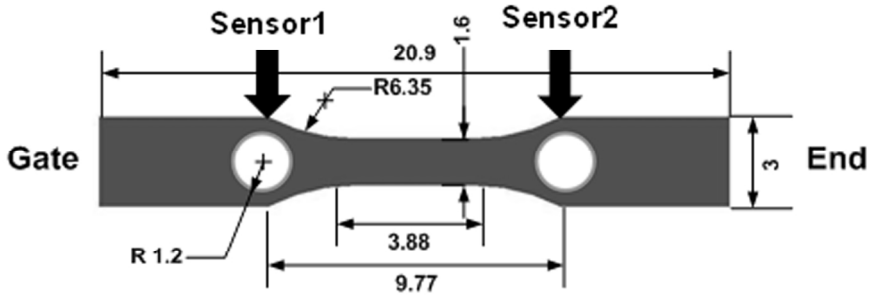

Figure 1: Mold and part: (d) dimensions of molded part (all in mm).
129x52mm (300 x 300 DPI)

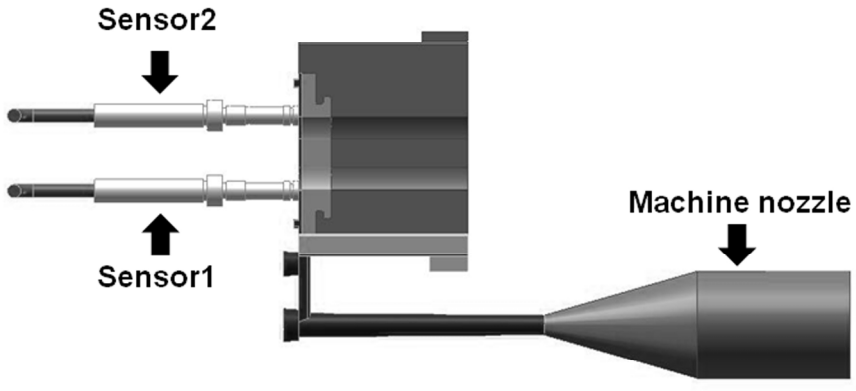

Figure 2: Process monitoring system: (a) melt delivery system with PT sensors
208x132mm (300 x 300 DPI)

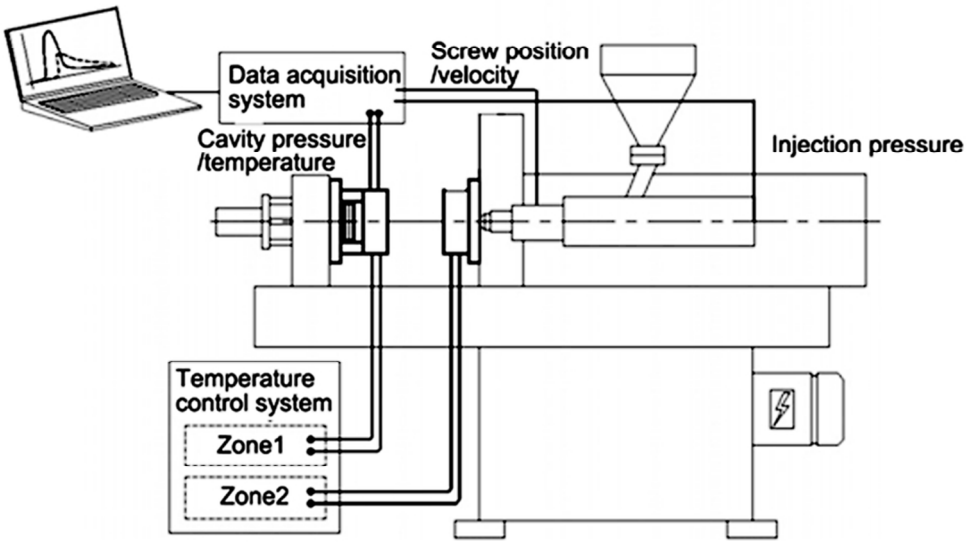

Figure 2: Process monitoring system: (b) data acquisition system
40x25mm (600 x 600 DPI)

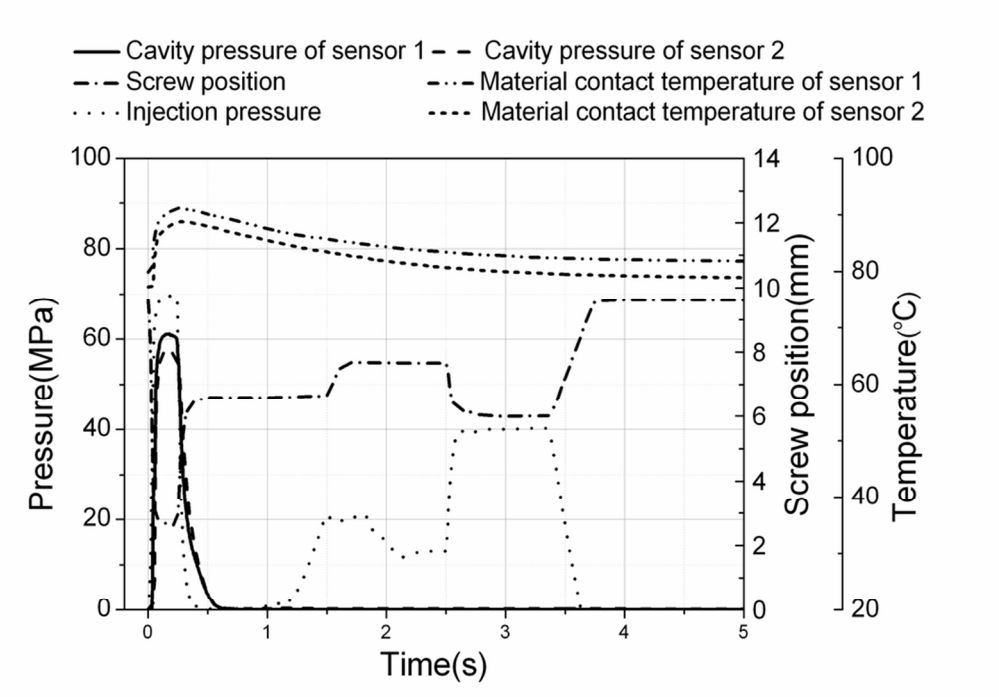

Trace curves of screw position, injection pressure, cavity pressure and material contact temperature of HDPE
44x31mm (600 x 600 DPI)

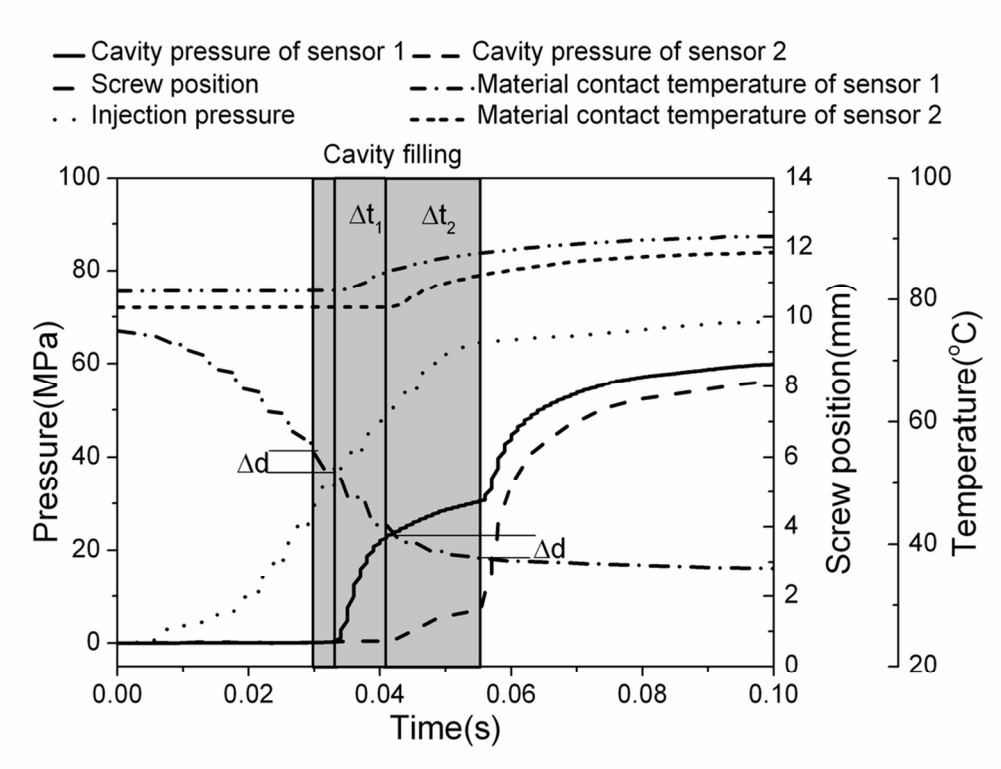

Figure 4: Trace curves of screw position, injection pressure, cavity pressure and material contact temperature within 0.1s
48x37mm (600 x 600 DPI)

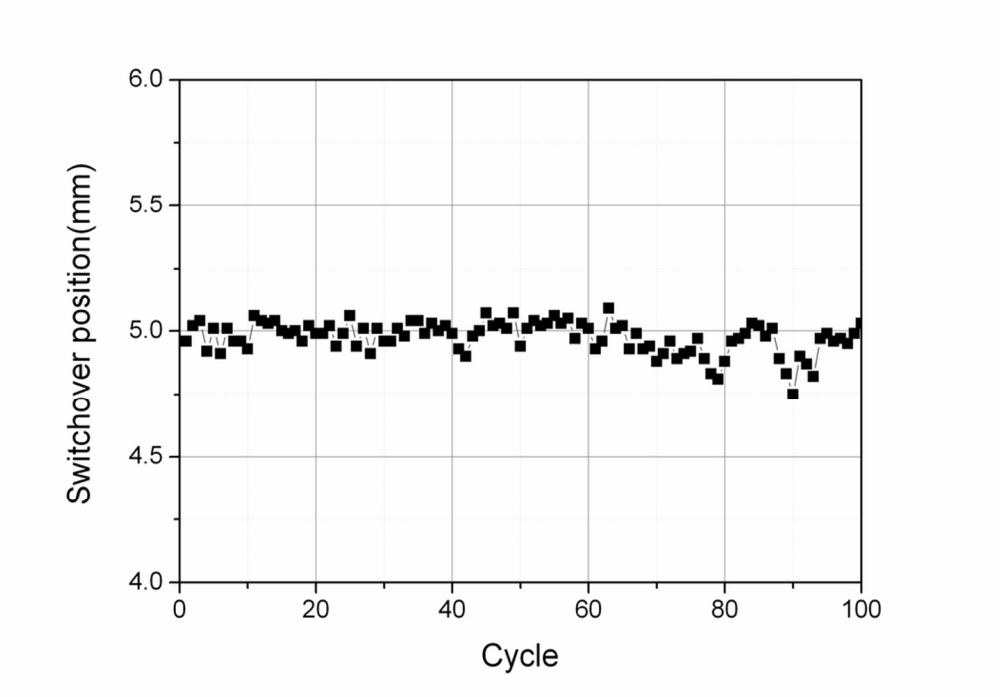

Figure 5: Actual switchover positions of 100 cycles
44x31mm (600 x 600 DPI)

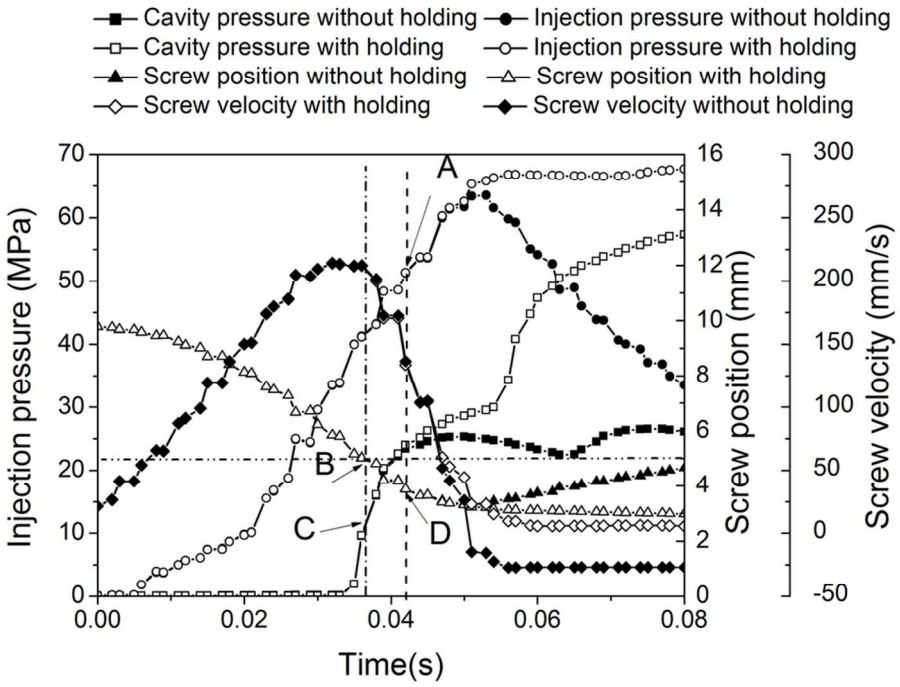

Figure 6: Profiles of cavity pressure, injection pressure, screw position and screw velocity for process condition 10 with and without packing pressure
44x31mm (600 x 600 DPI)

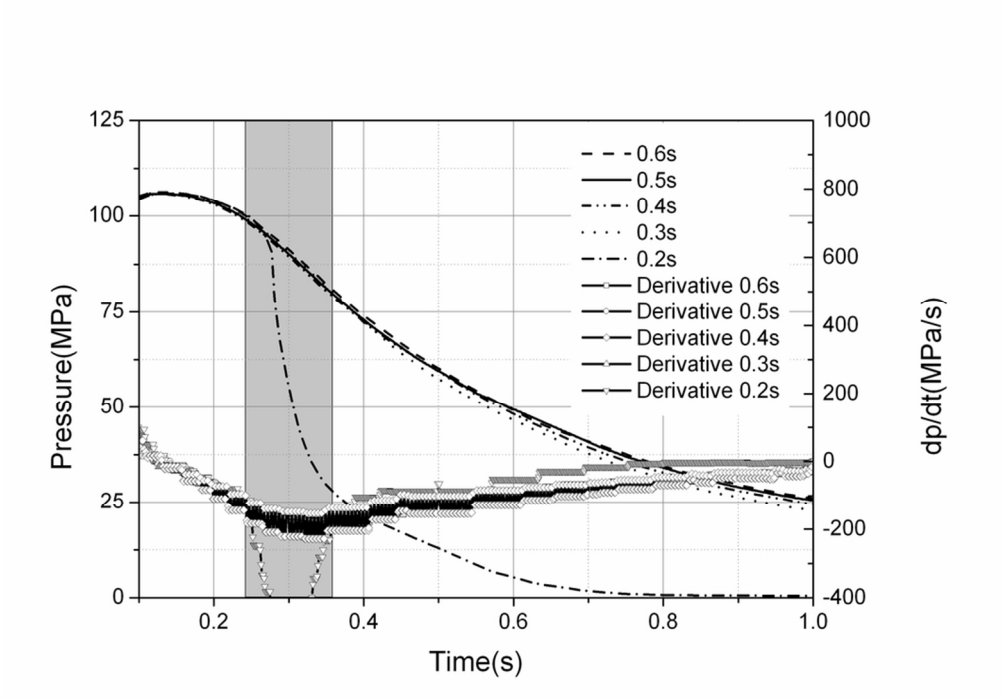

Figure 7: Gate solidification time estimation: (a) cavity pressure curves and their derivatives with different holding time
44x31mm (600 x 600 DPI)

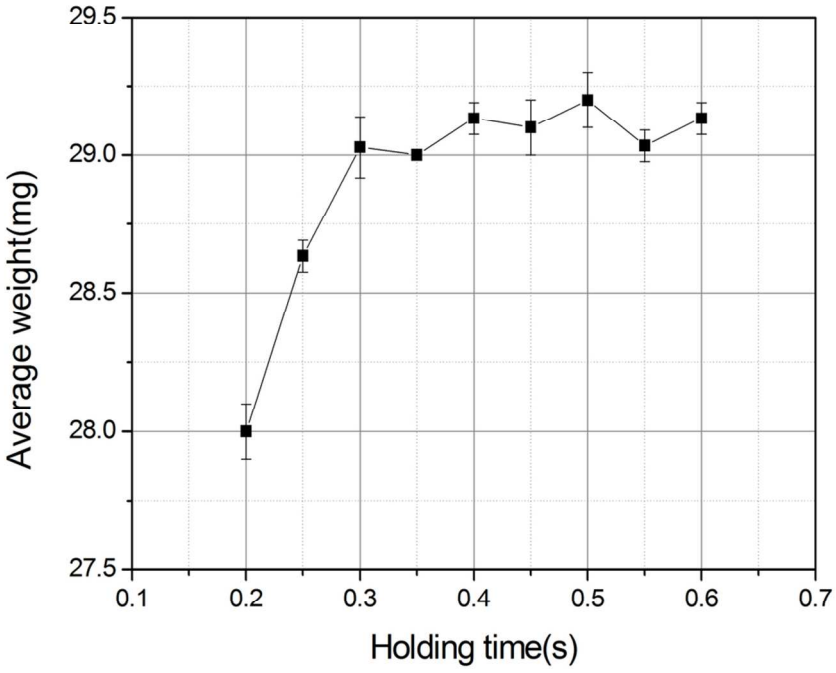

Figure 7: Gate solidification time estimation: (b) weight of parts at different holding time
48x37mm (600 x 600 DPI)

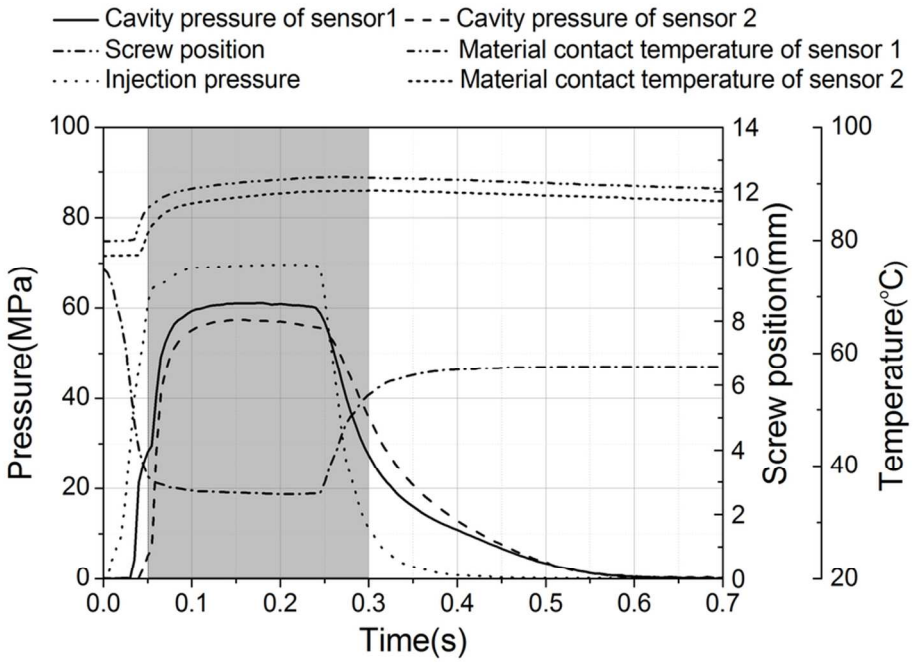

Figure 8: Trace curves of screw position, injection pressure, cavity pressure, and material contact temperature at post filling stage (holding stage is as per the shaded grey box)
44x31mm (600 x 600 DPI)

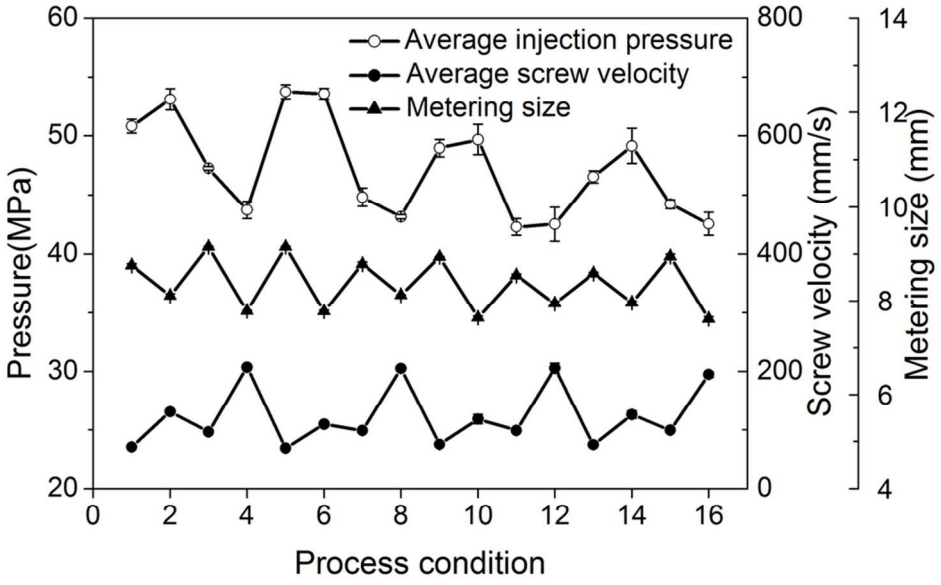

Figure 9(a): Variation of PCVs in filling process
44x31mm (600 x 600 DPI)

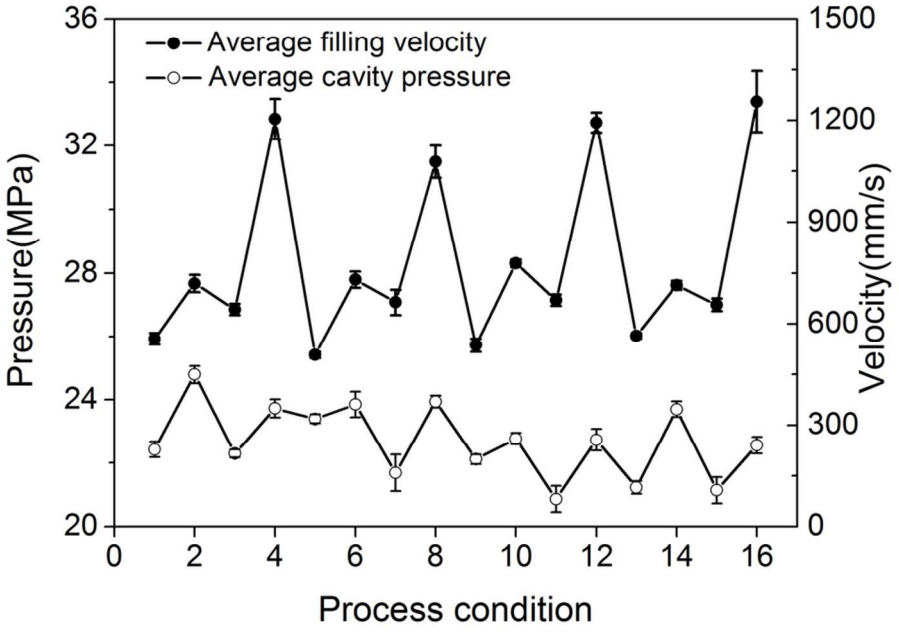

Figure 9(b): Variation of PCVs in filling process
44x31mm (600 x 600 DPI)

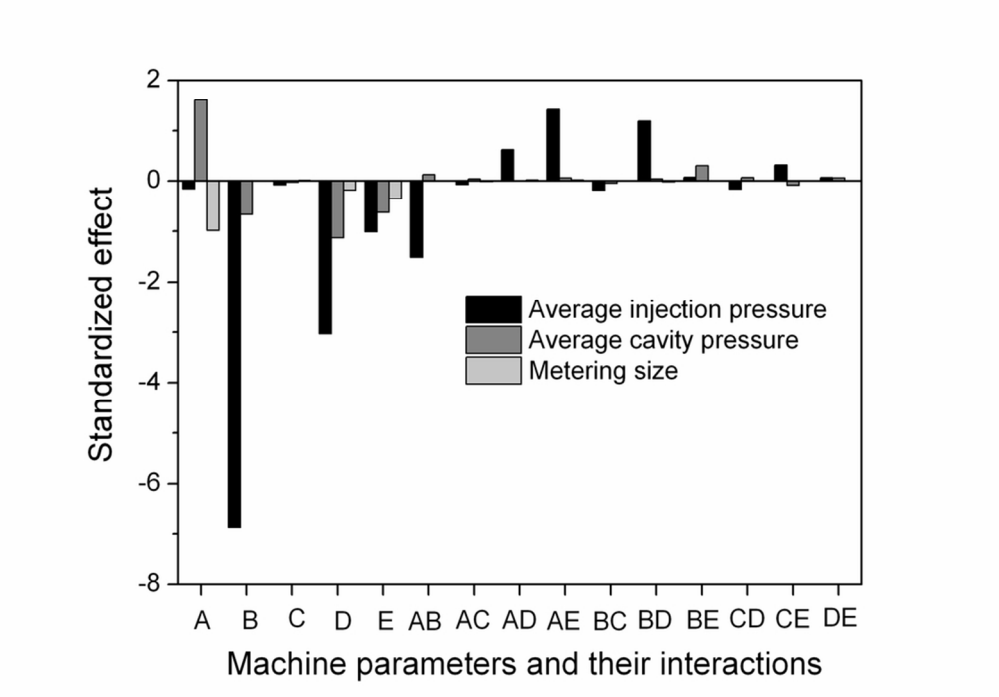

Figure 10(a): Standardized effects of the machine parameters and their interactions on PCVs in filling process (Parameters A=Vi, B=Ph, C=th, D=Tb, E=Tm (c.f. Table 1))
44x31mm (600 x 600 DPI)

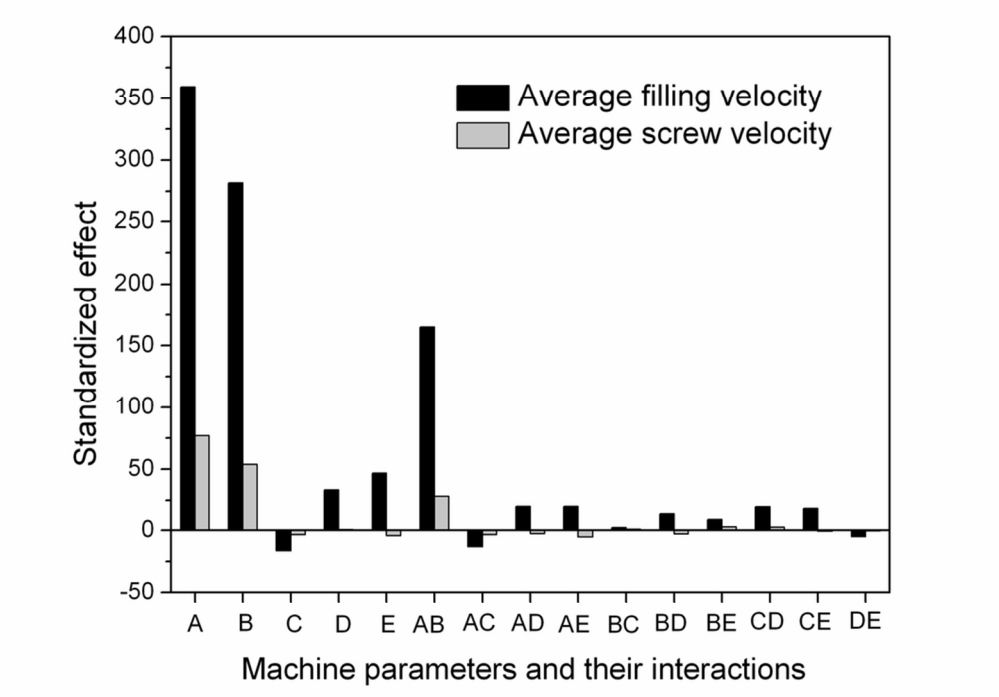

Figure 10(b): Standardized effects of the machine parameters and their interactions on PCVs in filling process (Parameters A=Vi, B=Ph, C=th, D=Tb, E=Tm (c.f. Table 1))
44x31mm (600 x 600 DPI)

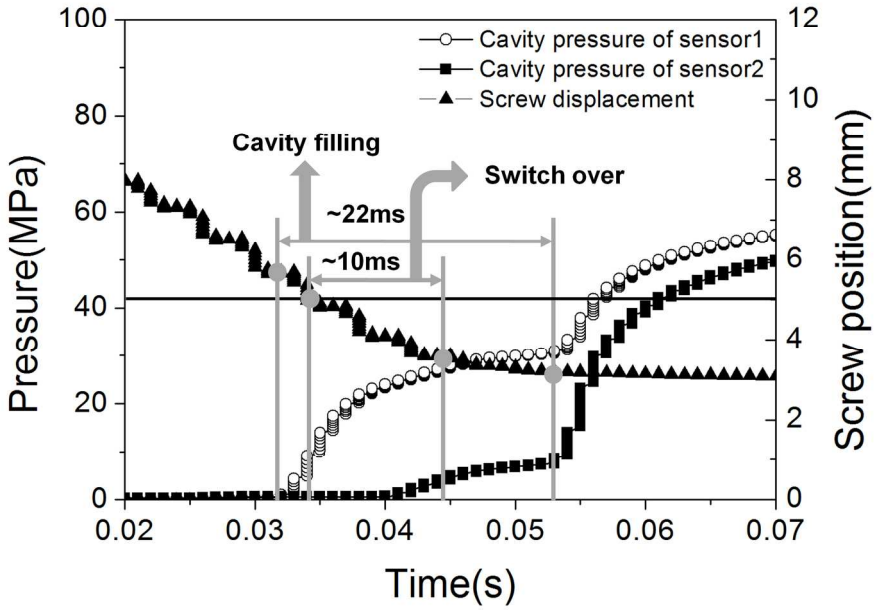

Figure 11: Effect of holding pressure on filling behavior: (a) process condition 10
190x142mm (300 x 300 DPI)

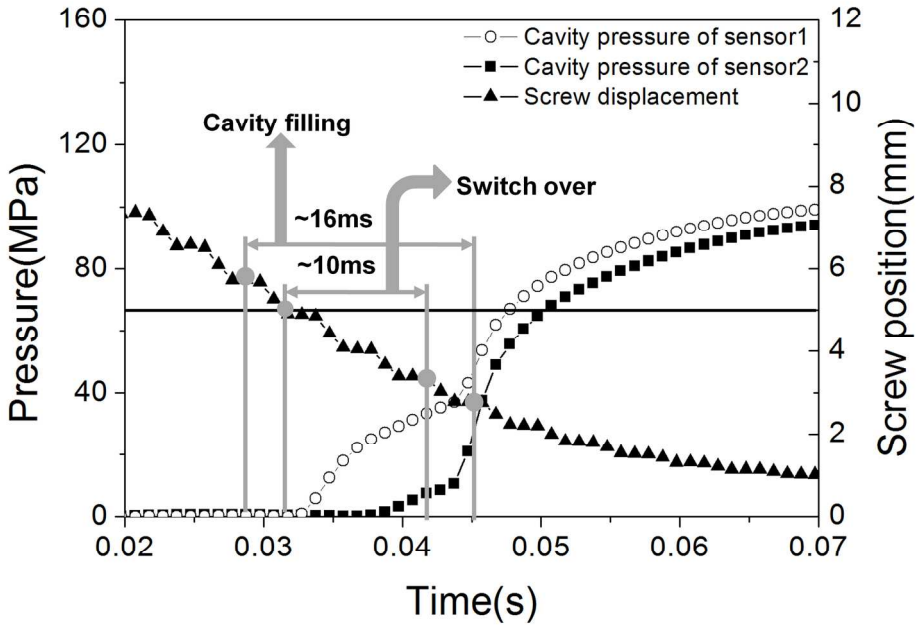

Figure 11: Effect of holding pressure on filling behavior: (b) process condition 16
190x142mm (300 x 300 DPI)

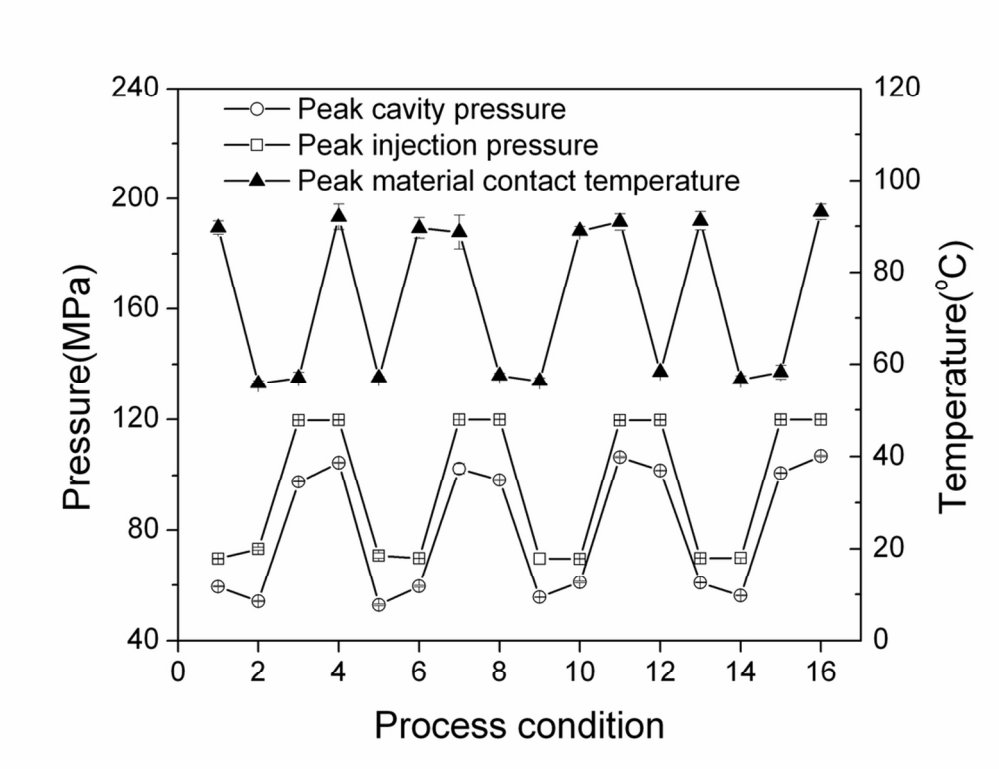

Figure 12(a): Variation of PCVs in post-filling process
48x37mm (600 x 600 DPI)

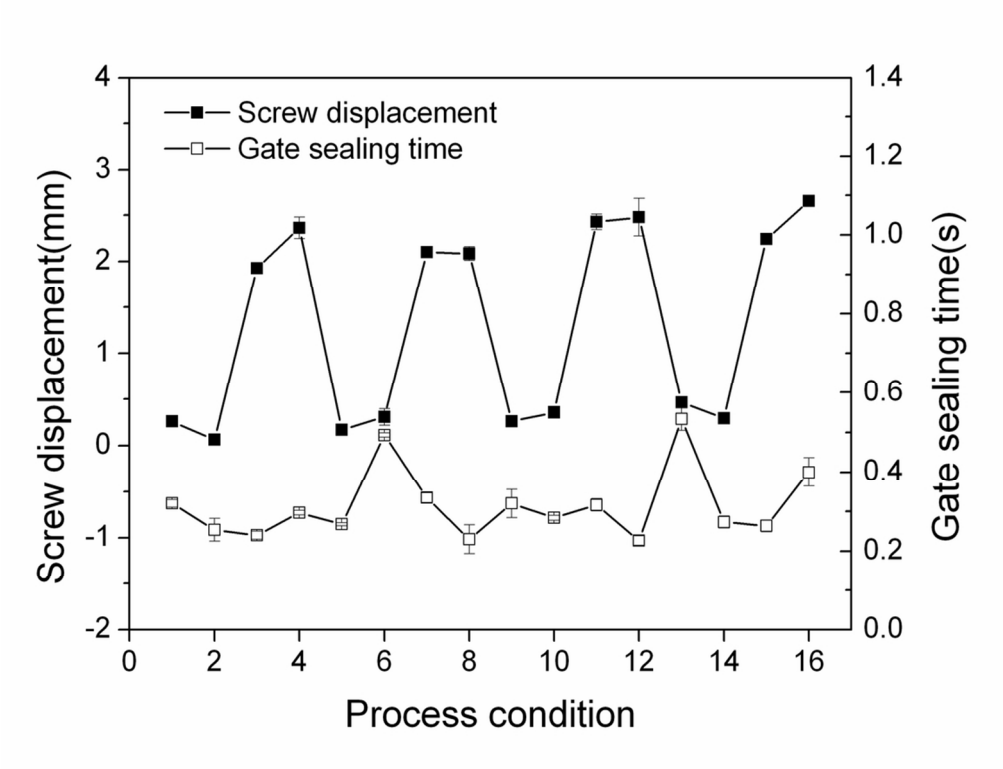

Variation of PCVs in post-filling process
48x37mm (600 x 600 DPI)

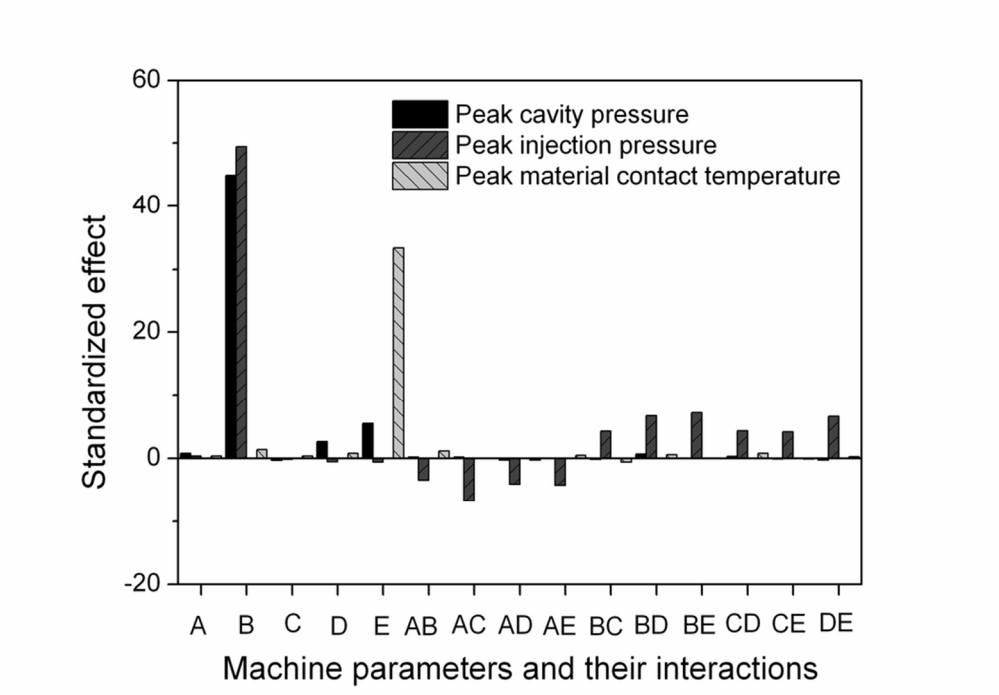

Figure 13(a): Standardized effects of the machine parameters and their interactions on PCVs in post-filling process (Parameters A=Vi, B=Ph, C=th, D=Tb, E=Tm (c.f. Table 1))
44x31mm (600 x 600 DPI)

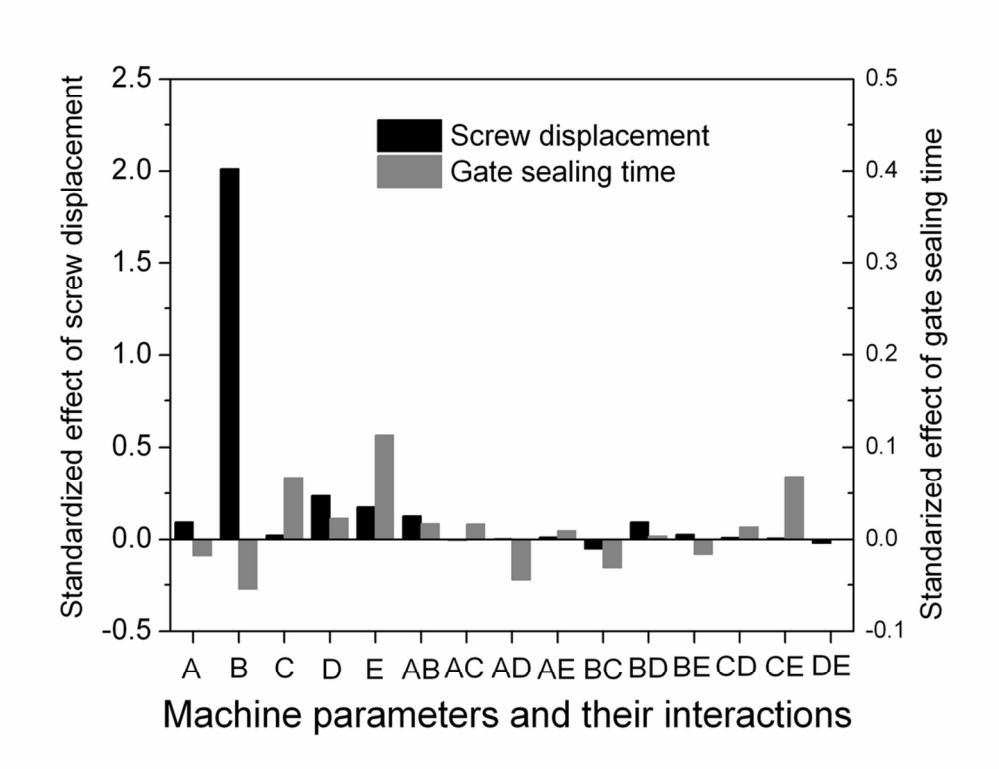

Figure 13(b): Standardized effects of the machine parameters and their interactions on PCVs in post-filling process (Parameters A=Vi, B=Ph, C=th, D=Tb, E=Tm (c.f. Table 1))
48x37mm (600 x 600 DPI)

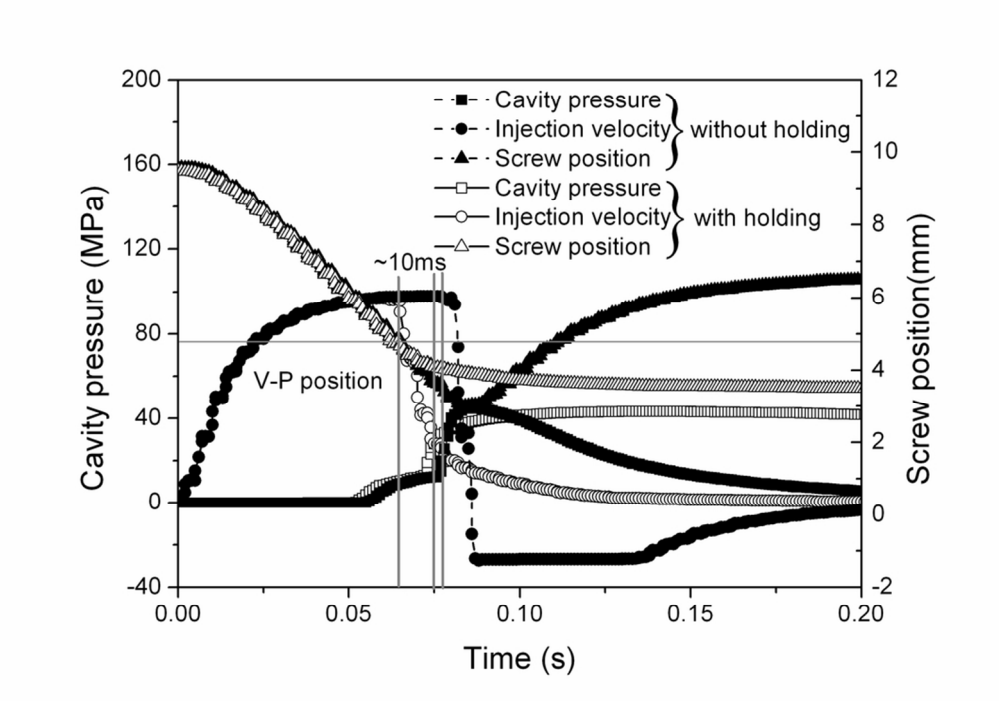

Figure 14: Full shot with and without holding stage after shot size optimization
44x31mm (600 x 600 DPI)

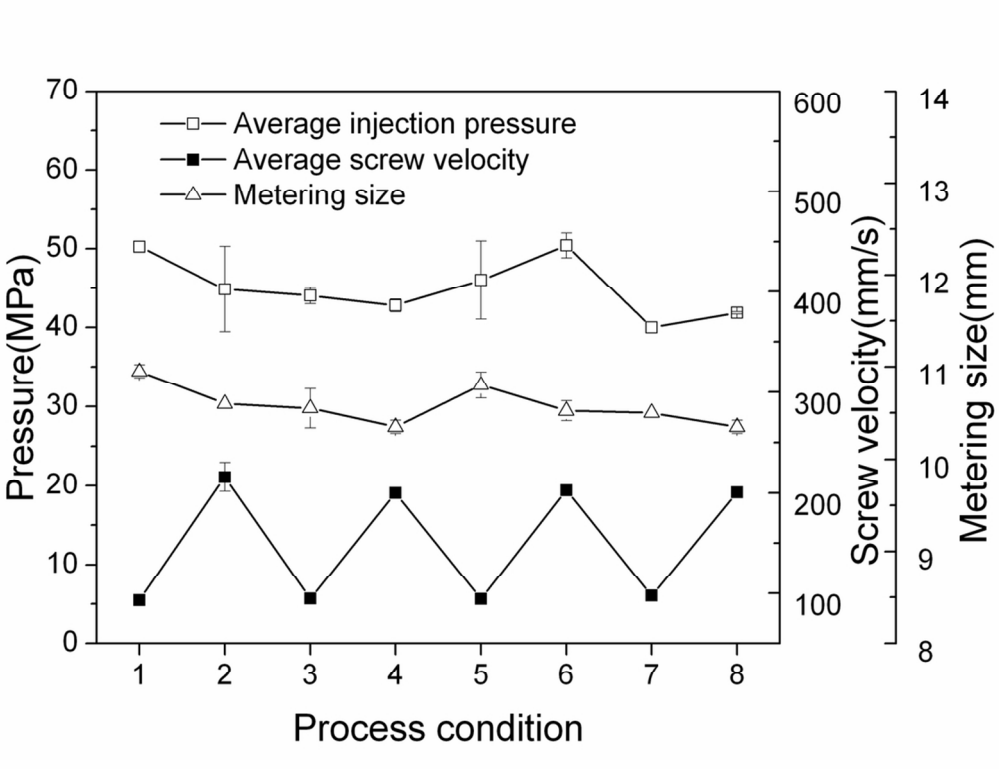

Figure 15(a): Variation of PCVs in filling process for COC
48x37mm (600 x 600 DPI)

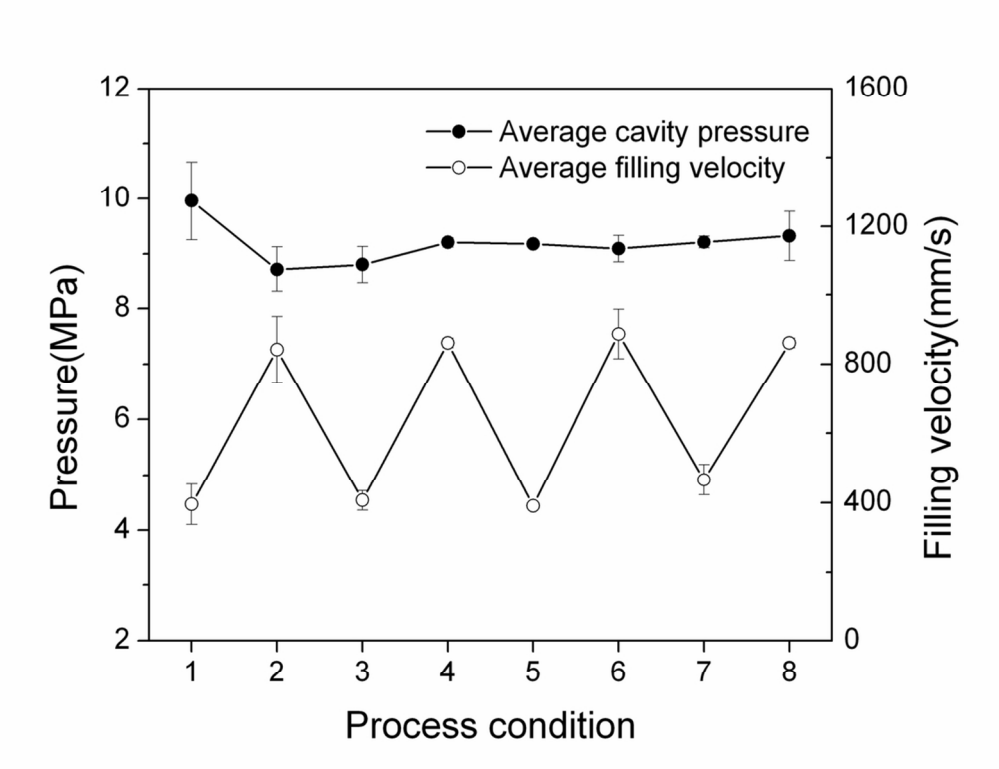

Figure 15(b): Variation of PCVs in filling process for COC
48x37mm (600 x 600 DPI)

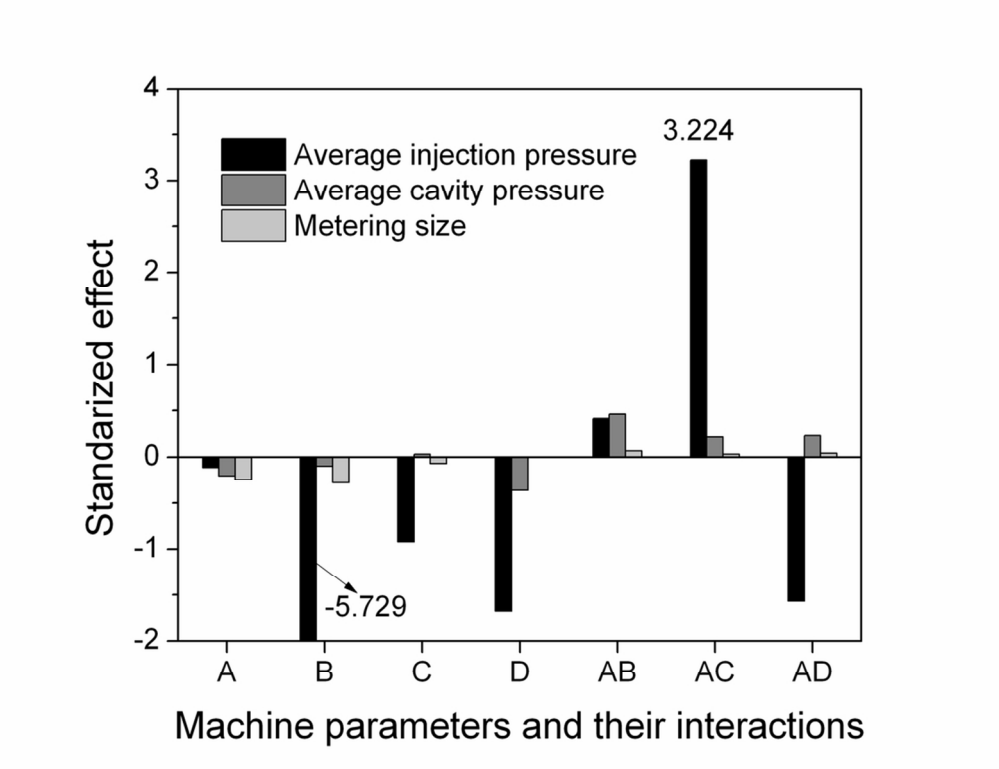

Figure 16(a): Standardized effects of the machine parameters and their interactions on PCVs in filling stage of COC (Parameters A=Vi, B= Tm, C=Ph, and D=th (c.f. Table 1))
48x37mm (600 x 600 DPI)

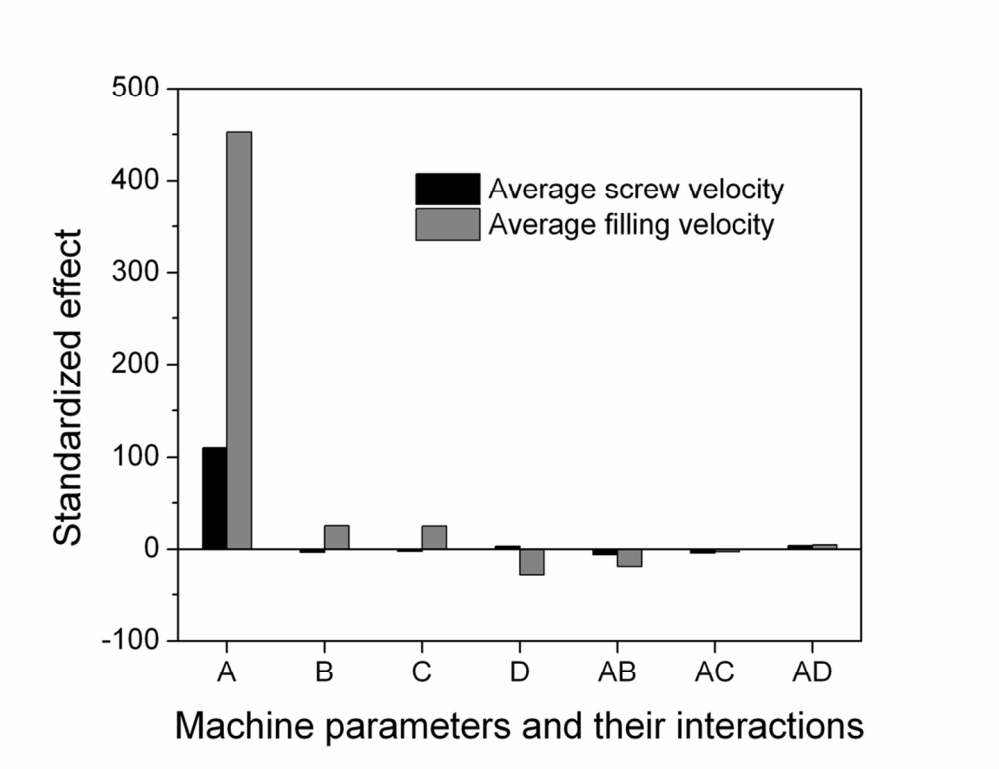

Figure 16(b): Standardized effects of the machine parameters and their interactions on PCVs in filling stage of COC (Parameters A=Vi, B= Tm, C=Ph, and D=th (c.f. Table 1))
48x37mm (600 x 600 DPI)

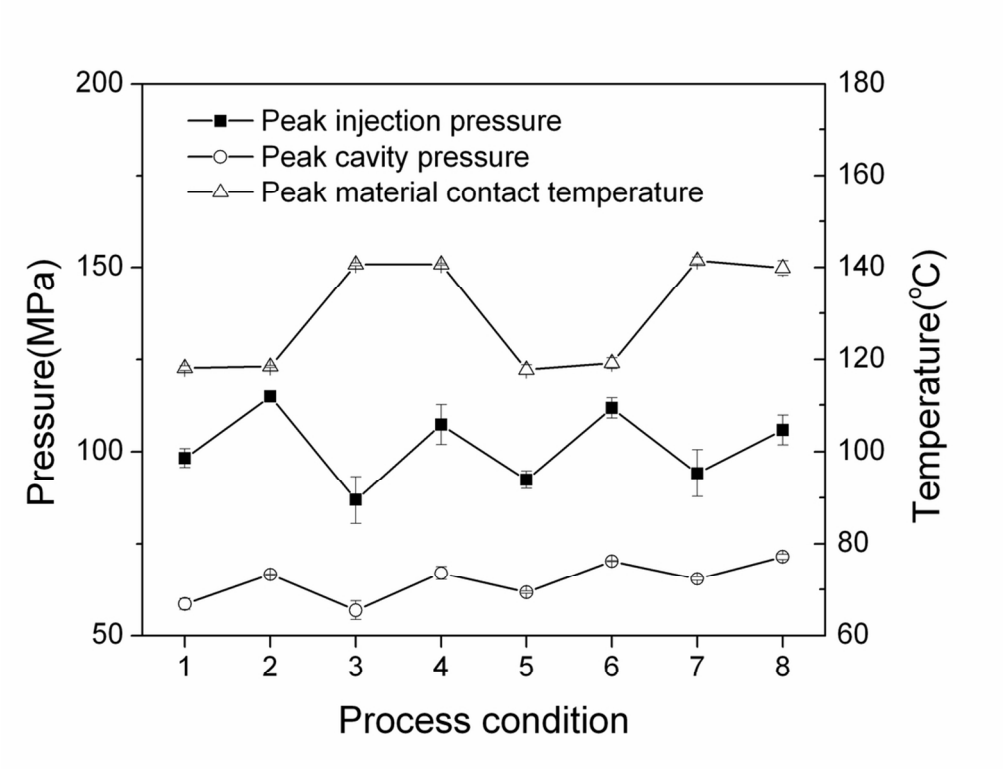

Figure 17(a): Variation of PCVs in post-filling process for COC
48x37mm (600 x 600 DPI)

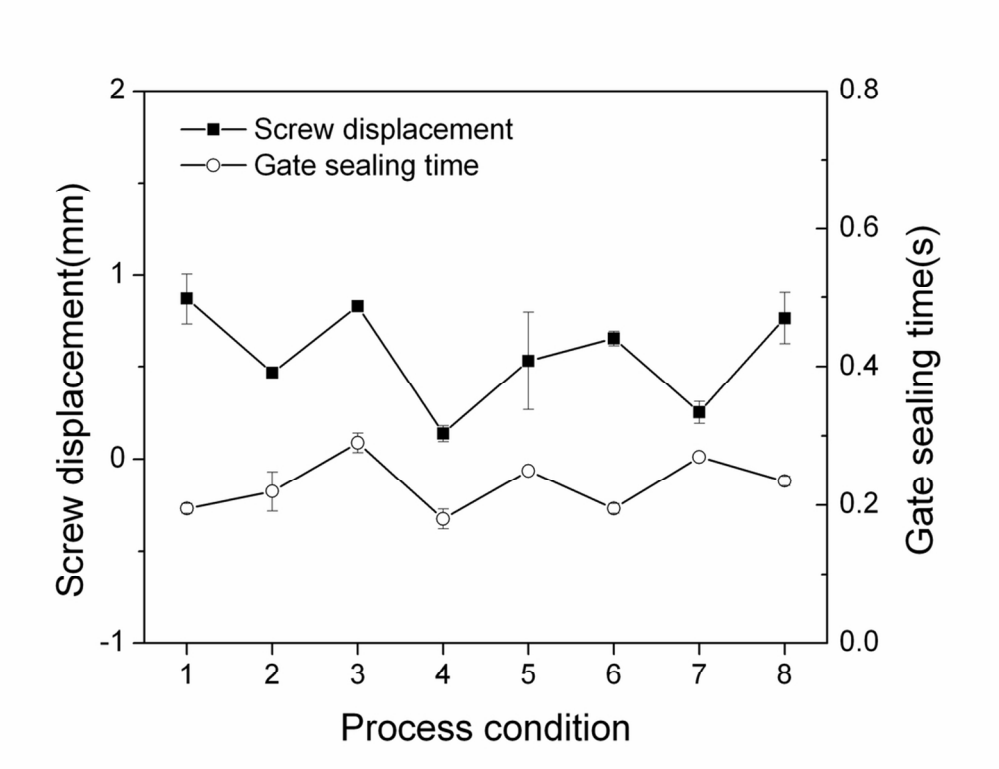

Figure 17(b): Variation of PCVs in post-filling process for COC
48x37mm (600 x 600 DPI)

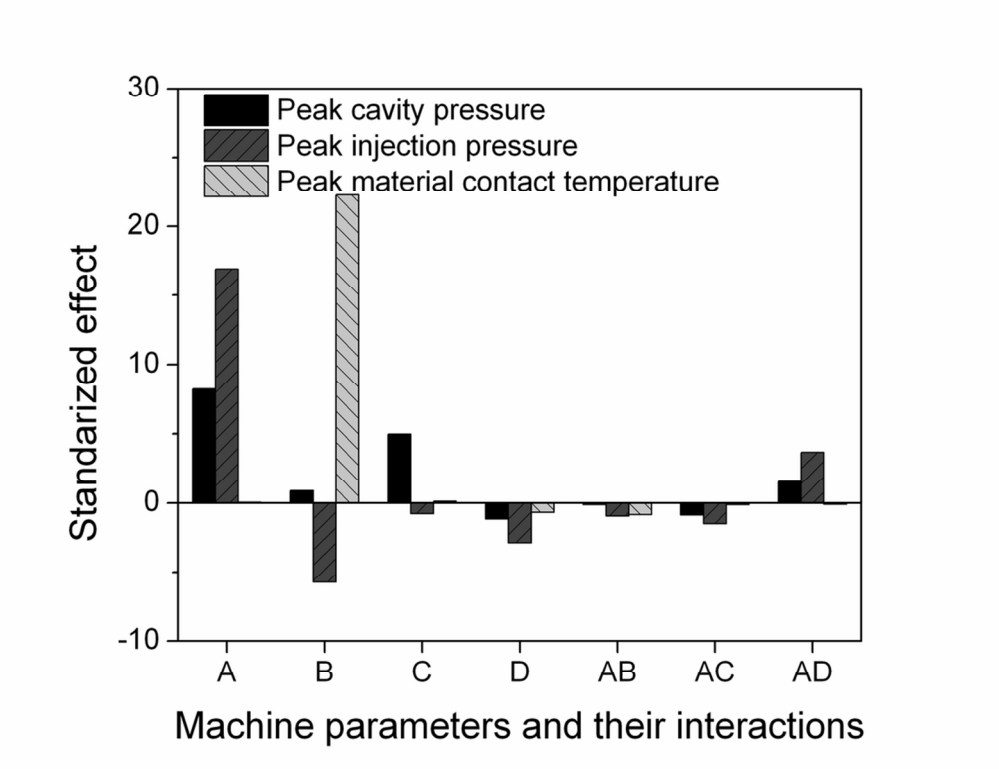

Figure 18(a): Standardized effects of the machine parameters and their interactions on PCVs in post- filling stage of COC (Parameters A=Vi, B= Tm, C=Ph, and D=th (c.f. Table 1))
48x37mm (600 x 600 DPI)

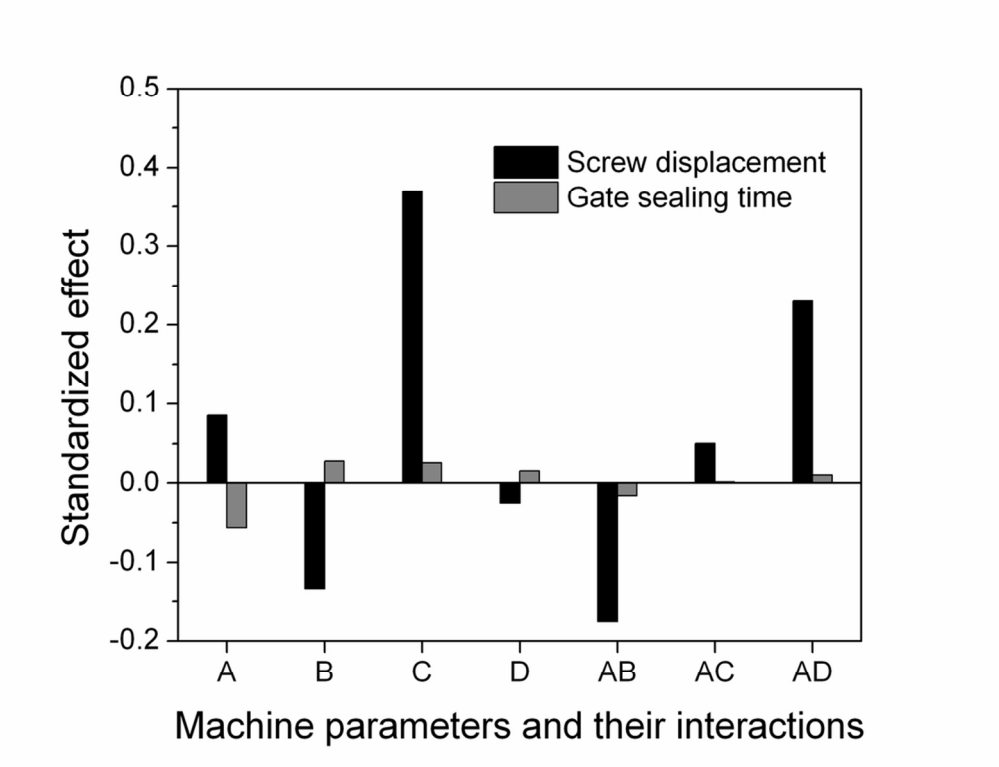

Figure 18(b): Standardized effects of the machine parameters and their interactions on PCVs in post- filling stage of COC (Parameters A=Vi, B= Tm, C=Ph, and D=th (c.f. Table 1))
48x37mm (600 x 600 DPI)